The Thesis Committee for Christopher Hancheng Chen
Certifies that this is the approved version of the following thesis:

Synthesis of Top Coat Surface Treatments for the Orientation of Thin Film Block Copolymers

APPROVED BY
SUPERVISING COMMITTEE:

Supervisor:

C. Grant Willson

Christopher J. Ellison

Synthesis of Top Coat Surface Treatments for the Orientation of Thin Film Block Copolymers

by

Christopher Hancheng Chen, B.S.; M.S.

Thesis

Presented to the Faculty of the Graduate School of

The University of Texas at Austin

in Partial Fulfillment

of the Requirements

for the Degree of

Master of Arts

The University of Texas at Austin

August 2013

Dedication

To my family for their unconditional love and support

Acknowledgements

The best decision I have made in my career was to join Professor C. Grant Willson's research group. Professor Willson is more than just an amazing advisor. He is a true mentor and someone that I aspire to grow and mature to be. His patient guidance over the past years has developed me as not only a researcher but as a person. I am truly fortunate to have had the opportunity to work with him. Professor Christopher Bielawski was another important component of my graduate career at the University of Texas at Austin as he offered invaluable help with the direction of my research. I would also like to thank Professor Christopher Ellison for being a part of my committee and providing so much advice over the past years.

Graduate school would not have been the same without the support and care from my fraternity brothers in Professor Willson's research group. William Durand, it was the best of times, it was the worst of times to share a hood with you. We work great together as a team, but we sure do pile up a lot of dirty glassware. Will has been a great colleague and friend, making my time at UT unforgettable (in a good way). Logan Santos, thank you for looking after me even after you graduated. Dr. Michael Jacobsson, although our time in the research group only overlapped for a few semesters, you gave me timeless advice about graduate school. Ryan Mesch, thank you for the late night help for preparing my thesis. I would also like to thank the rest of my group: Michael Maher, Dr. Christopher Bates, William Bell, Dr. Xinyu Gu, Ryan Deschner, Dr. Hao Tang, Greg Blachut, Andrew Dick, Colin Hayes, Austin Lane, and Philip Liu. I must also acknowledge the undergraduates, who bring so much charisma and character to our research group: Leon Dean, Anthony Thio, and Wade Wang.

There are so many other people at the University of Texas at Austin for whom I am grateful. The Bielawski group has also been important to my graduate career. I had the opportunity to work with Jonathan Moerdyk, a brilliant chemist and collaborator. John Brantley has given me so much support while at UT. One day, you will have that lecture hall where you can sit in front of a fireplace and talk about chemistry. Many current and former members of the Bielawski group deserve my gratitude: Dr. Rob Ono, Garrett Blake, Dr. Dan Varnado, Dr. Brent Norris, Dr. Kelly Wiggins, Dr. Beth Neilson, Eric Silver, Alex Todd, Dr. Dan Dreyer, Daphne Sung, and Christopher Johnson. The chemistry graduate office has been an invaluable part of my time at UT. Penny Kile has kept me from missing more deadlines than I can remember and has kept me on track during my entire time at UT.

Finally, I want to thank dK for your unconditional support and encouragement. This would have all been different without you.

Abstract

Synthesis of Top Coat Surface Treatments for the Orientation of Thin Film Block Copolymers

Christopher Hancheng Chen, M.A.

The University of Texas at Austin, 2013

Supervisor: C. Grant Willson

Block copolymer self-assembly has demonstrated sub-optical lithographic resolution[1]. High values of χ, the block copolymer interaction parameter, are required to achieve next-generation lithographic resolution[2]. Unfortunately, high values of χ can lead to thin film orientation control difficulties[3], which are believed to be caused by large differences in the surface energy of each block relative to the substrate and the free surface. The substrate-block interface can be modified to achieve a surface energy intermediate to that of each individual block[4]; the air-polymer interface, however, presents additional complications. This thesis describes the synthesis of polymers for top coat surface treatments, which are designed to modify the surface energy of the air-block copolymer interface and enable block copolymer orientation control upon thermal annealing. Polymers with β-keto acid functionality were synthesized to allow polarity switching upon decarboxylation. Syntheses of anhydride containing polymers were established that provide another class of polarity switching materials.

Table of Contents

List of Figures

Chapter 1: A History of Hard Disk Drives and Customer Demand

Microchips have evolved over time; their minimum features have steadily decreased in size, thereby increasing the density of wires and transistors enabling higher data capacity and faster speed. These dramatic improvements in integrated circuits were necessary to follow the unceasing growth in consumer demand for smaller, faster, and cheaper microchips. In 1965, Gordon Moore, the co-founder and eventual CEO of Intel Corporation, plotted the course of the evolution of microchips:

> *"The complexity for minimum component costs has increased at a rate of roughly a factor of two per year…over the longer term, the rate of increase is a bit more uncertain, although there is no reason to believe it will not remain nearly constant for at least 10 years."*[5]

This projection, known as Moore's Law, details a doubling in the number-density of transistors on an integrated circuit every 18-24 months[6]. Figure 1.1 portrays the striking accuracy of Moore's prediction since 1960.

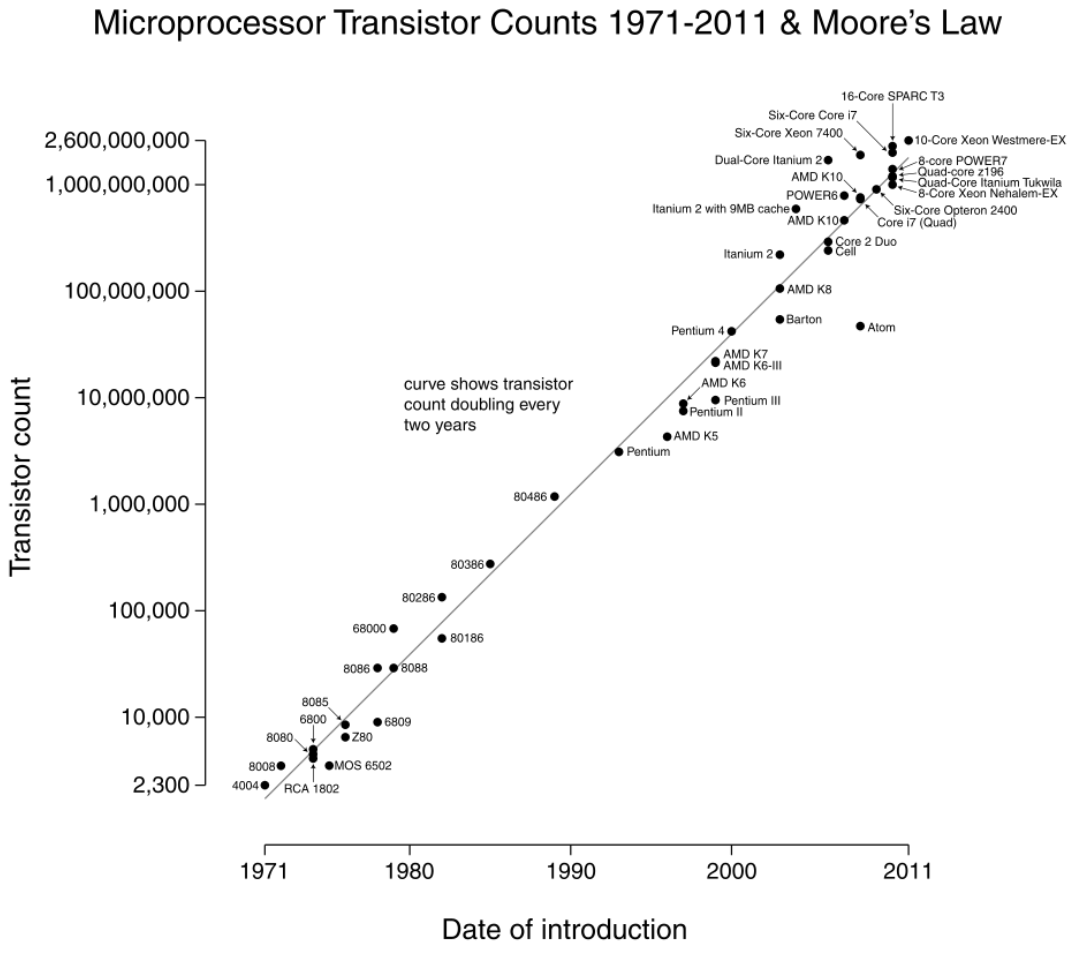

Figure 1.1. Plot of microprocessor transistor counts against dates of introduction[7]

To follow the trend of increasing transistor density, innovations are required in chemistry, engineering, and physics. Specifically, the improvements in microelectronic performance are driven by advances in the field of photolithography and nano-patterning techniques. These processes, which involve patterning materials using physical and chemical transformations, must continually improve the minimum patternable dimensions to keep pace with the demands of the microelectronic industry. One particular subset of the microelectronic industry that demands the greatest improvements in

patterning capabilities has been within the hard disk drive industry, where next-generation devices are created using the smallest possible dimensions (Figure 1.2).

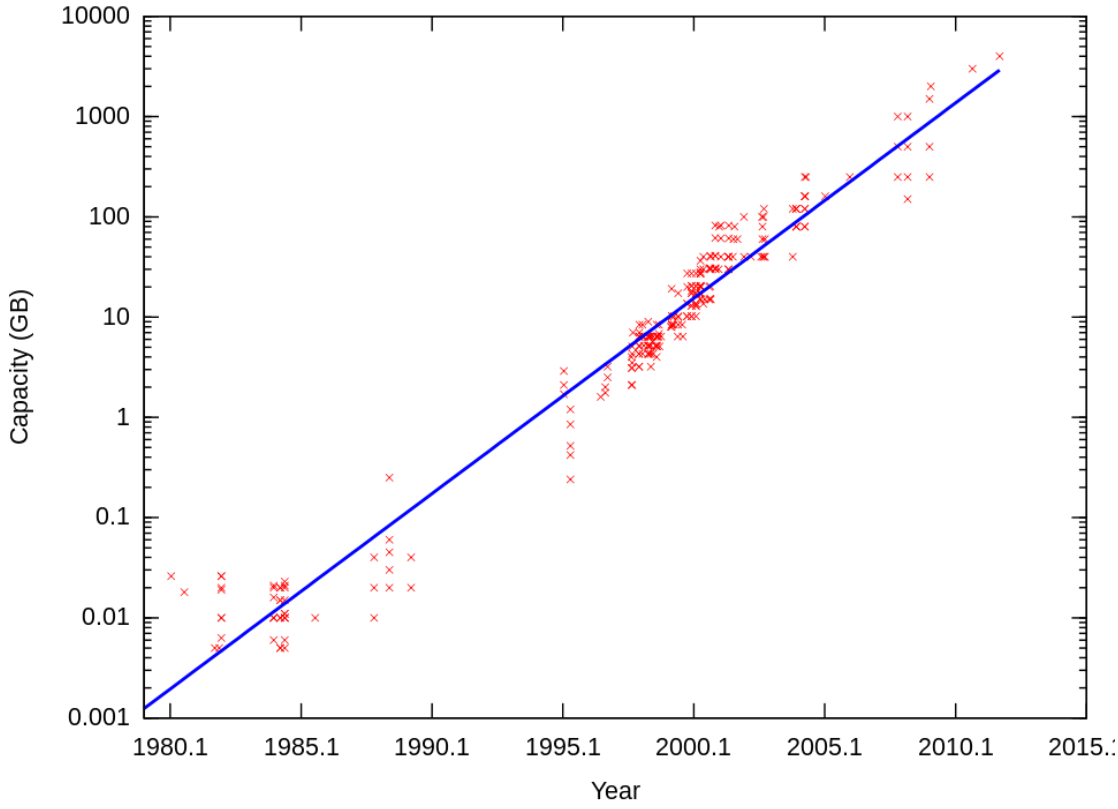

Figure 1.2. Plot of hard disk drive capacity since 1980[8]

The storage capacity of these next-generation hard disk drives is directly related to the minimum patternable dimensions using lithographic processes. The improvements in storage density of the hard disk drives would not have been possible without advancements in the materials used to create them.

Hard drives are stacks of disks covered in magnetic material referred to as grains.

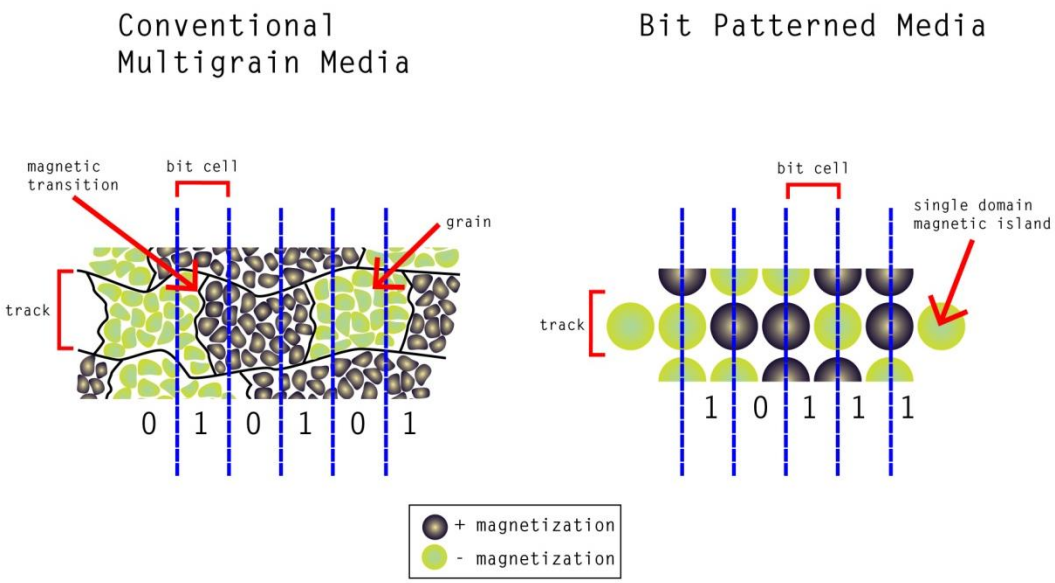

Figure 1.3. Conventional multigrain media (left) and bit patterned media (right). From Chen, Stefanie, "Conventional Multigrain Media and Bit Patterned Media" December 5, 2012 via http://www.stuffbystef.com. Reprinted with permission from Stefanie Chen[9]

Within the concentric tracks of the disk, the read-write head passes over the grains and writes the information by magnetizing regions of ferromagnetic material on the disk. Within the track, a transition in the magnetic polarization is classified as a digital "1" of the binary bit (Figure 1.3). A lack of magnetic polarization change in the predetermined location of the bit cell is defined as a digital "0" in the bit. The sequence of "1's" and "0's" then become the binary code by which computers store data. To meet pace for demands of higher capacity storage media, the areal density of hard disk drives must be increased by decreasing the sizes of the bit cells.

There are, however, two issues that limit the extent to which the size of a bit cell may be decreased: signal-to-noise issues and superparamagnetism. In order to maintain a good signal-to-noise ratio, the bit boundaries must be well-defined within random

clusters of magnetized grains. Rough boundaries around the bit cell, caused by difficulties in the write head creating well-defined sections, produce noise. As the size of the bit cells are decreased by decreasing the number of grains per bit cell, the boundaries become less clear and noise increases. The other option to increase areal density is to decrease the size of the grains. Superparamagnetism, however, limits the size to which the grains can be minimized. Their magnetic polarization has a certain amount of thermal instability that is limited by the size and volume of the grain, causing the grains to spontaneously flip their magnetization under the influence of neighboring fields. At a certain point, the grains can no longer hold the magnetization and store the data from the write head. The most recent advances in conventional multigrain media have achieved a maximum of 667 Gbit/in^2 for the hard drive storage capacity[10]. A new approach must be taken to increase the areal density of hard disk drives while maintaining archival data security.

One proposed solution that may surpass the 1 Tbit/in^2 limit is through bit patterned media. Unlike conventional multigrain media, bit patterned media has discrete domains separated by non-ferromagnetic material (Figure 1.3), which can act as single-switching volumes. This effectively removes the signal-to-noise issues in the continuous domains of conventional multigrain media. The superparamagnetic effect is essentially circumvented because a single bit cell can be decreased to a single grain. Bit patterned media, however, has not yet been implemented into industrial scale manufacturing processes, because a fully functioning patterning technique is not available to produce the isolated domain features at the required size to meet data density needs.

Chapter 2: Photolithography and Directed Self Assembly of Block Copolymers

Photolithography is the conventional process used to pattern substrates for microelectronic devices. As seen in Figure 2.1, optical lithography is a multistep procedure. A photoresist, a light-sensitive material that shows resistance to specific etch conditions, is spin-coated onto a substrate. Certain regions of the photoresist are then exposed to light through a mask, which renders the exposed regions soluble to developer (positive tone) or less soluble to developer (negative tone). A developer is used to create relief patterns in the photoresist that provide patterning access to the substrate material. The relief pattern is then transferred into the substrate using carefully selected etch conditions that show higher selectivity for the substrate over the photoresist. The photoresist is then stripped leaving the desired features in the substrate. Further processing steps are then used to fabricate the multilayer devices that will act as microchips.

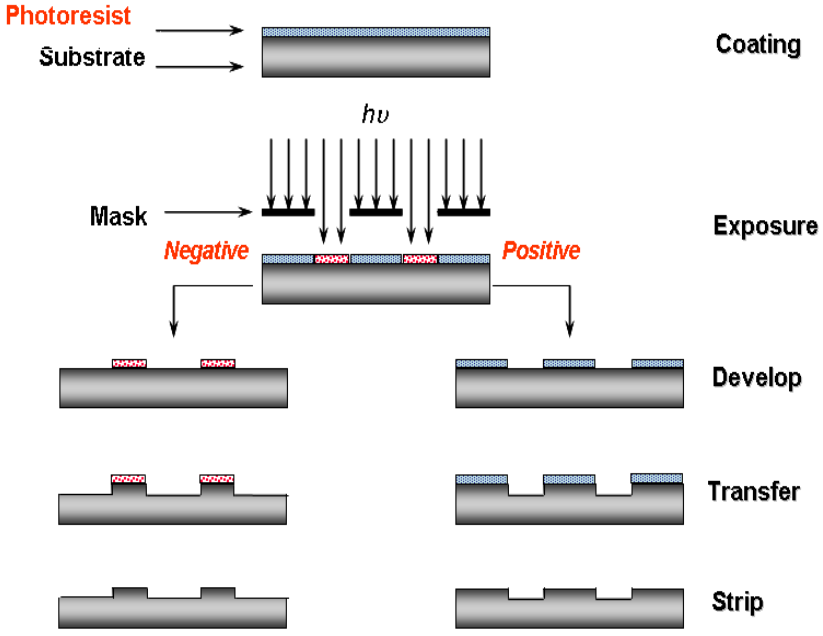

Figure 2.1. The optical lithography process[11]

Currently, optical lithography has reached its resolution limit of 34 nm as all of the factors governing the resolution described in Rayleigh's equation below have been optimized.

$$R = \frac{k_1 \cdot \lambda}{NA}$$

Here, R is the minimum resolution of a feature, k_1 is a resist dependent factor, λ is the emission wavelength of light from the exposure source, and NA is the numerical aperture of the lens[11]. The resist dependent factor, k_1, is currently around 0.3, close to the theoretical limit of 0.25[12]. NA, which includes the refractive index of the material between the lens and substrate and the acceptance angle of the lens, is now at 1.44 in water immersion lithography. Further improvements to the acceptance angle are not possible and all efforts to find a high index liquid to replace water have failed. The most efficient light source utilized today generates 193 nm light from an ArF excimer laser, and no bright and reliable shorter-wavelength light source has yet been demonstrated. With these parameters, the resolution limit is 34 nm. Attempts are being made to decrease the wavelength of light by converting to extreme ultraviolet (EUV), which is supposed to provide 13.5 nm light, but doing so requires very costly equipment[13]. The 34 nm limit can be circumvented with such techniques as double patterning, but this approach is time consuming and expensive due to its extra processing steps. Since 27 nm full-pitch is required for 1 Tb/in^2 hard drive storage capacity, an alternative route must be taken to obtain smaller resolution.

One solution to the limitations of conventional photolithography is imprint lithography. Imprint lithography is a cheap, high-throughput process that uses a master template to directly mold in the photoresist on the substrate (Figure 2.2). The patterned

photoresist is treated in a manner similar to that used in optical lithography processes to transfer the pattern into the substrate.

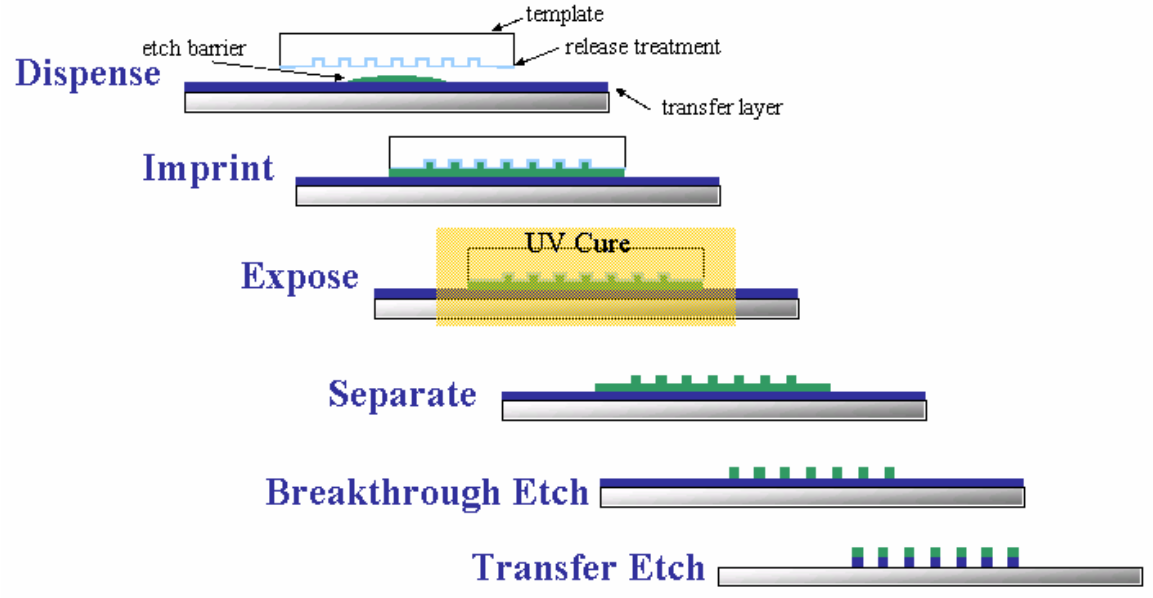

Figure 2.2. The nanoimprint lithography process[14]

The resolution of nanoimprint lithography is only restricted by the mold structure. Features as small as 2.4 nm have been replicated portraying the high resolution capability of nanoimprint lithography[15]. However, such high resolution techniques as electron-beam lithography are required for making the master template. Electron-beam lithography, a serial and relatively slow process, is estimated to take several weeks and cost over $1 million to fabricate an imprint template necessary to reach industry targets for future bit-patterned microelectronic devices[16]. Thus, a solution that can efficiently improve the patterning throughput and/or resolution in an inexpensive manner would be valuable for the production of next-generation bit-patterned microelectronic devices.

The great versatility of self-assembling block copolymers (BCP) makes them a promising candidate to allow the microelectronics industry to continue its trend towards

smaller features over the next decade [17,18]. Block copolymers, two homopolymers that are covalently bonded, can self-assemble on the nanoscopic length scale in a variety of morphologies and sizes. BCPs can be applied onto a substrate, will self-assemble when annnealed, and then one of the blocks can be removed with a selective etch process. The remaining nanoscopic pattern can then be transferred into the substrate. As shown in Figure 2.3, multiple variables can be fine-tuned to adjust the outcome of the self-assembly: the chi interaction parameter (χ), the degree of polymerization (N), and the volume fraction (f)[19]

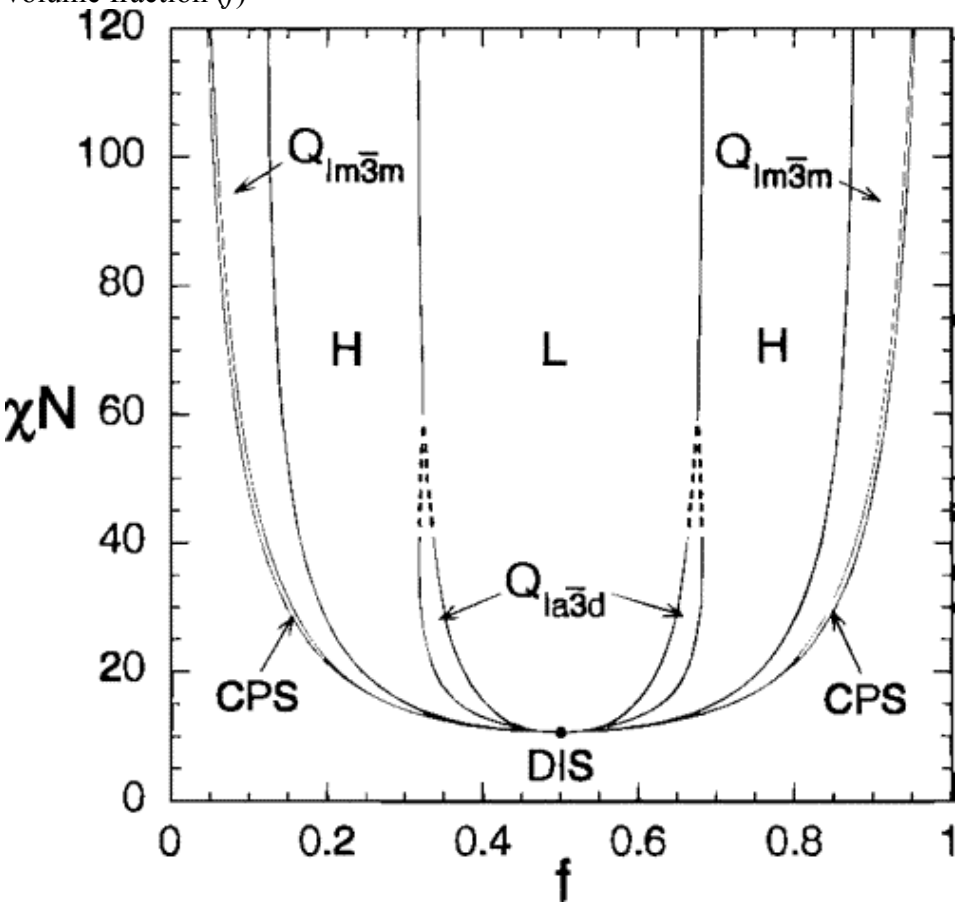

Figure 2.3. Phase diagram of block copolymer self-assembly. Phase are labeled L (lamellar), H (hexagonally packed cylinders), $Q_{Ia\bar{3}d}$ (bicontinuous Ia$\bar{3}$d cubic), $Q_{Im\bar{3}m}$ (bcc spheres), CPS (close-packed spheres), and DIS (disordered).[20]

An important issue for industry adoption of BCP patterning is the controlled orientation of the polymer structures[21]. A number of factors influence the orientation: film thickness[22], substrate topology, and interfacial interactions of the film. In addition, a large Flory-Huggins interaction parameter (χ) is required to allow formation of small feature sizes[23]. Unfortunately, larger χ values tend to be accompanied by block domains with large surface energy differences, thus resulting in difficulties in controlling the orientation.

Silicon-containing block copolymers often possess high χ[24] and allow for the selective removal of one block with oxygen reactive ion etching. Oxygen etching removes the organic material and leaves the silicon-containing features as a silicon dioxide etch mask. Unfortunately, many of these polymers, such as poly(styrene-*block*-dimethylsiloxane)[25], suffer from mismatched block-air surface energies. The silicon-containing block often aligns parallel to the substrate so that the lower surface energy block can be preferentially exposed to the air interface. Cross-linked surface coatings applied to the substrate have been shown to aid in controlled orientation of self-assembled block copolymers by minimizing the surface free energy at the substrate interface (neutral condition)[26]. However, the large surface energy differences between blocks of most high-χ BCPs with air will induce horizontal orientation even in the presence of a neutral substrate interface. Therefore, a top surface layer that can minimize the surface energy at the top interface can enable vertical alignment of high-χ materials. An illustration of the effect of the influence of surface energy on the orientation of BCPs is shown in Figure 2.4.

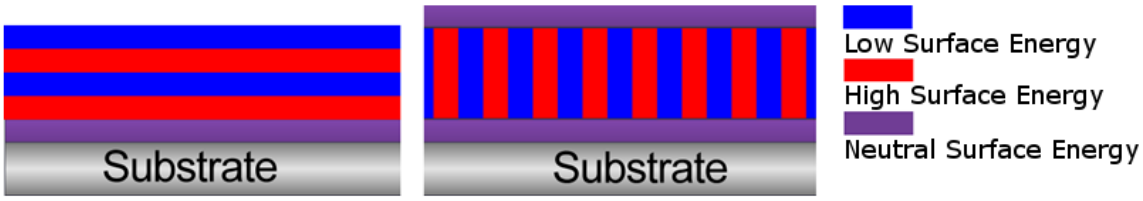

Figure 2.4. Effect of surface treatments on the orientation of high-χ BCPs. With the presence of the air interface, only horizontal features are observed. A neutral top interface allows for the vertical orientation of the block domains.

The importance of a neutral top interface is critical for the orientation of high-χ materials, but the same methods employed to minimize the surface energy at the substrate interface are not amenable for the top. Thus, materials that can be deposited onto the top interface of the BCP and provide a neutral surface energy are desired.

Chapter 3: Surface Energy Switchable Top Coats

The hard disk drive industry is very experienced and well-equipped to spin coat a large variety of polymers; therefore, the ideal top coat deposition method is to directly spin coat them onto the BCP. The main hurdle for a spin coated top coat is being able to deposit it onto the block copolymer without dissolving it. Typical polymers that are soluble in orthogonal solvents such as water often have very high surface energies; thus, it is difficult to find polymers matching the surface energy of the block copolymers (typically low surface energy). To circumvent this problem, a new type of top coat with a switchable surface energy was designed. This top coat could be deposited from a polar solvent and through a polarity switch (i.e., polar to non-polar) can form a neutral interface with a surface energy between that of the two blocks, as illustrated in Figure 3.1.

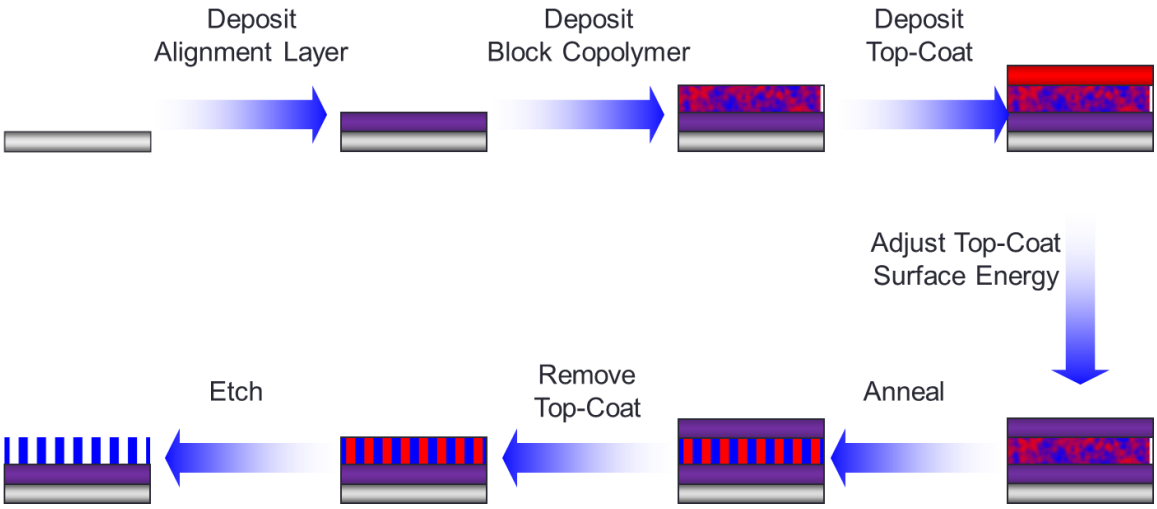

Figure 3.1. Procedure for substrate preparation with a high-χ silicon-containing block copolymer and a spin coated top coat.

In addition to a polarity switch mechanism, the top coat surface treatment requires a scaffold that can be easily modified to vary its polarity. The neutral surface energy to

obtain perpendicular alignment of the block copolymer will vary depending on the block copolymer[27,28]. Another necessary characteristic of the top coat is a high glass transition temperature[29]. The block copolymer must be able to be thermally annealed above its Tg, while staying below the Tg of the top coat. This would allow a larger processing window and potentially shorter annealing times for Si-containing BCPs[29].

3.1. Addition Polymer of Norbornene

A material with a high T_g is the addition homopolymer of norbornene (T_g> 220 ^oC)[30,31]. An example top coat composed of a norbornene addition polymer with a pendant β-keto carboxylic acid functionality is illustrated in Figure 3.2. The β-keto carboxylic acid moiety should allow for aqueous base solubility and subsequently undergoes facile thermal decarboxylation to yield an acetate, which is less polar. This system has the potential to produce a neutral top coat from a water-soluble material. Additionally, the alpha position can be easily modified to change the polarity of the polymer following decarboxylation.

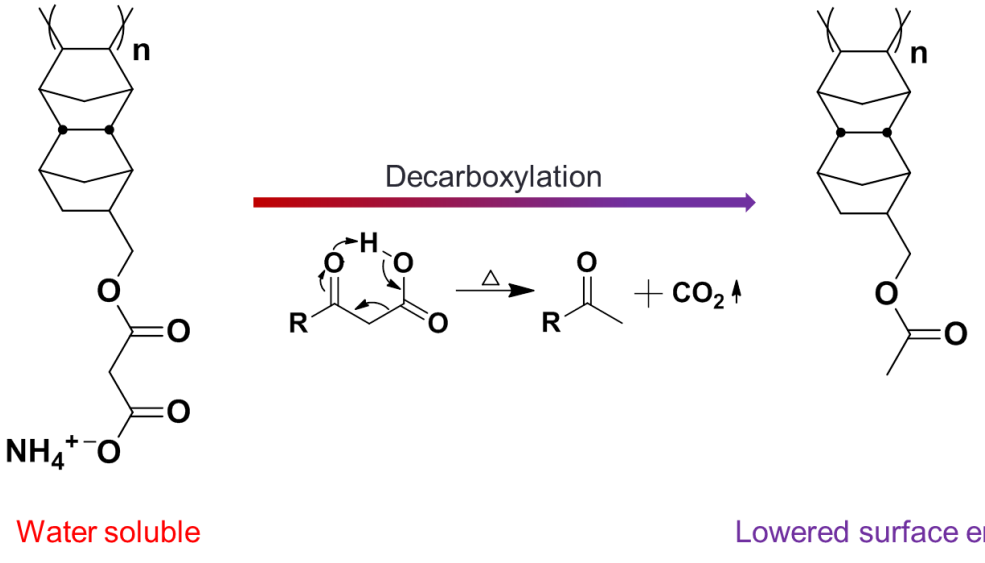

Figure 3.2. The β-keto acid functionality is converted to an acetate group following decarboxylation.

Initial work towards the top coat polymer in Figure 3.2 began with the synthesis of a norbornene monomer containing a β-keto ester functionality that would then be deprotected following polymerization (Figure 3.3).

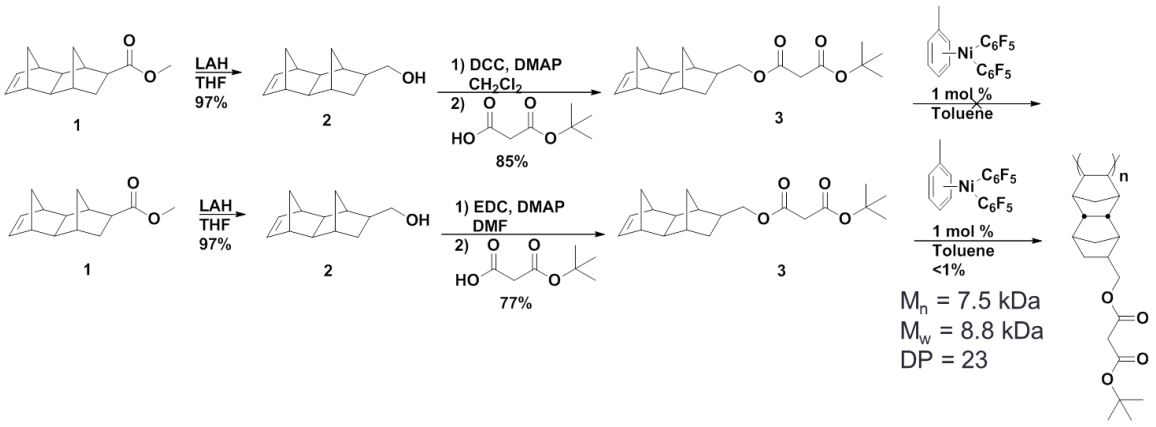

Figure 3.3. Synthesis of the target monomer from the commercially available dinorbornene methyl ester. Molecular weight of the polynorbornene complex was measured by gel permeation chromatography relative to a polystyrene standard.

The synthesis was conducted via a Steglich esterification with N, N'-dicyclohexylcarbodiimide (DCC) and dimethylaminopyridine (DMAP) as a catalyst in methylene chloride. The reaction yielded dicyclohexylurea (DCU) as a by-product, which was difficult to separate from the target compound. Numerous separations were attempted using column chromatography with silica gel; further attempts were conducted with basic alumina as the stationary phase and a variety of solvents for the mobile phase. DCU, however, was still present in the product following the attempted purifications. For this reason, the esterification was conducted with *N*-(3-Dimethylaminopropyl)-*N'*-ethylcarbodiimide hydrochloride (EDC) and DMAP. The urea byproduct of this reaction is easily removed by aqueous extractions. It is important to note that there was no reactivity of the starting materials when the reaction was conducted in methylene

chloride. The reaction proceeds with 77% yield when dimethylformamide is utilized as the solvent.

A metal catalyst, (η^6-toluene)Ni(C_6F_5)$_2$, polymerizes norbornene in high yields and molecular weights[32]. Unfortunately, the first synthesized monomer would not polymerize with the nickel catalyst (NiArF), presumably due to the dicyclohexylurea impurity that was so difficult to remove. Using EDC for the esterification produced the pure desired monomer, but it polymerized only in low yields and to low molecular weight.

The nickel catalyst is known to be water sensitive, so it was believed that the acidic protons in the alpha position of **3** might be inhibiting the polymerization. Therefore, the alpha position was dimethylated to remove the presence of acidic protons (Figure 3.4). The dimethylated compound, **4**, was synthesized but did not afford an efficient polymerization. Again, the yield was low and the degree of polymerization was low.

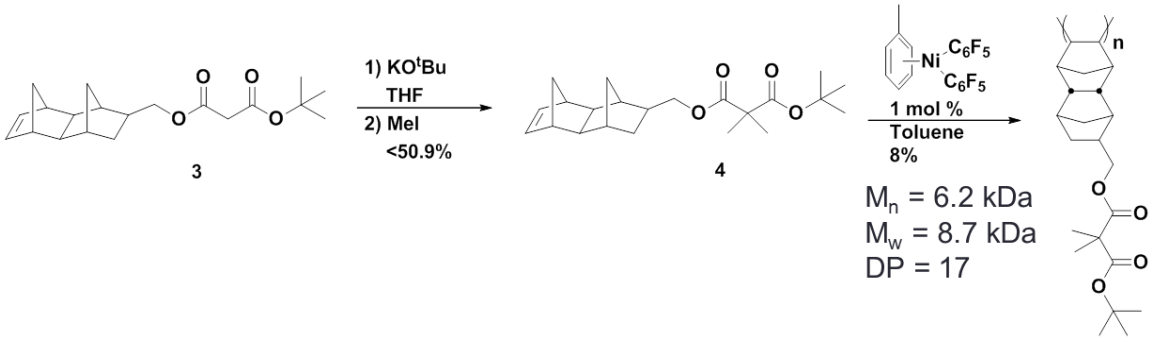

Figure 3.4. Synthesis of the target monomer appended with methyl groups to remove acidic protons.

This result led to a control study of NiArF to determine its compatibility with a 1,3-dicarbonyl functionality (Figure 3.5). Dimethyl malonate was dimethylated to remove acidic protons and the product was introduced into the polymerization of **1**. Increased

catalyst loadings had no effect on the yield of the polymerization. These results led to abandoning attempts to polymerize β-keto ester monomers. It is presumed the lack of polymerization is due to the chelation of the 1,3-dicarbonyl to nickel since Nickel(II) acetylacetonate is a known organometallic complex[33].

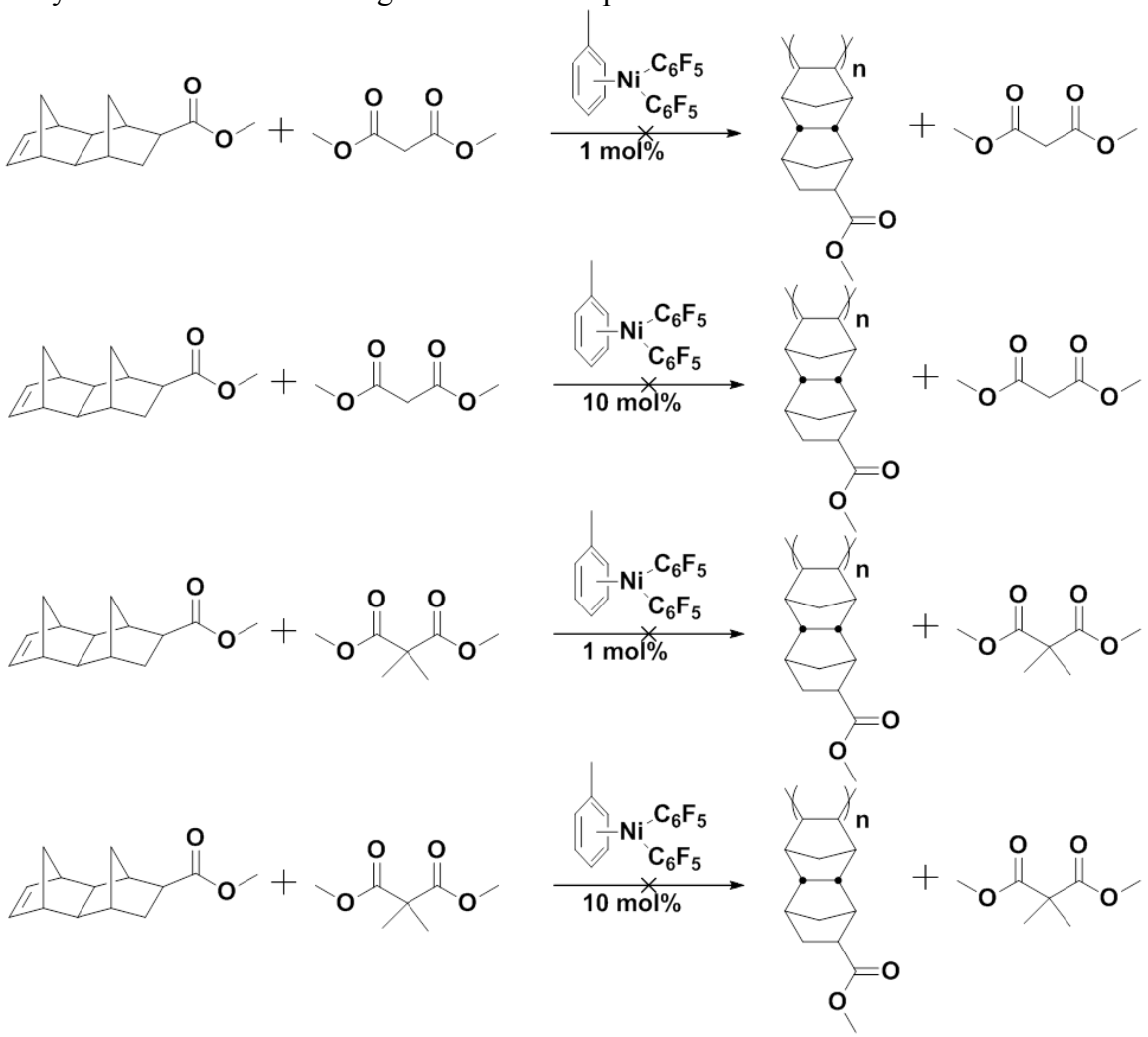

Figure 3.5. Control studies of the NiArF catalyst.

To avoid the di-carbonyl coordination problem, we pursued a post-polymerization modification towards the desired polymer (Figure 3.6). The dinorbornene methyl ester was polymerized with NiArF to afford the homopolymer **5**. A reduction of

the methyl ester with lithium aluminum hydride gave **6**. The yield of this reduction was difficult to reproduce in subsequent post-polymerization modifications. The alcohol product of the reduction was only soluble in DMF or DMSO. If the polymer was not fully converted to the alcohol quickly, it would precipitate in THF and stop the reduction. A Steglich esterification provided the protected malonate, **7**. The polymer was dissolved in a 1:1 mixture of trifluoroacetic acid and methylene chloride to obtain the homopolymer with the β-keto acid functionality, **8**. Dissolving the polymer in ammonium hydroxide resulted in a solution of **9** that could then be spin-coated onto the BCP. The polymer, however, was not readily soluble in aqueous base. The poor solubility may be attributed to partial decarboxylation of the polymer. Numerous issues were encountered with the conversion of the t-butyl ester to the carboxylic acid; These issues will be addressed in Chapter 3.3. After sonication in a 1:3 mixture of ammonium hydroxide and methanol for 2 hours, the heterogenous mixture was then filtered through a 0.2 μm polytetrafluoroethylene filter and spin-coated onto the BCP.

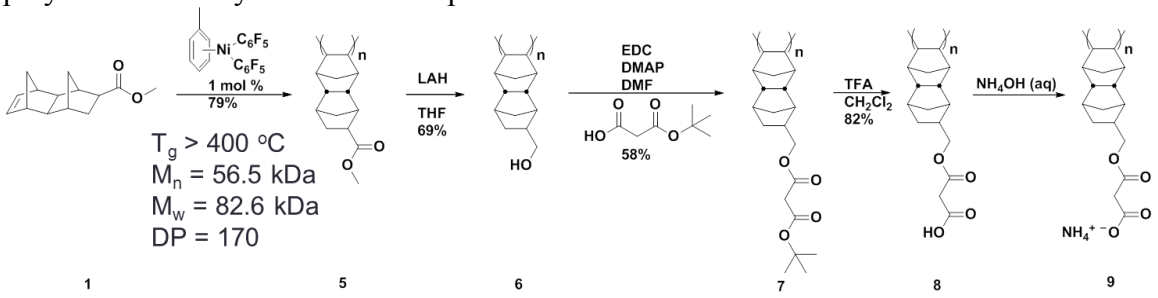

Figure 3.6. Synthesis of the addition polymer of dinorbornene with the the β-keto acid functionality via post-polymerization modification.

The β-keto acid polymer was tested by thermal gravimetric analysis to monitor the temperature of the decarboxylation (Figure 3.7). The weight loss observed upon decomposition (*ca* 150 °C) corresponds to loss of carbon dioxide. The change in weight before 100 °C is presumably due to mass loss of residual solvent.

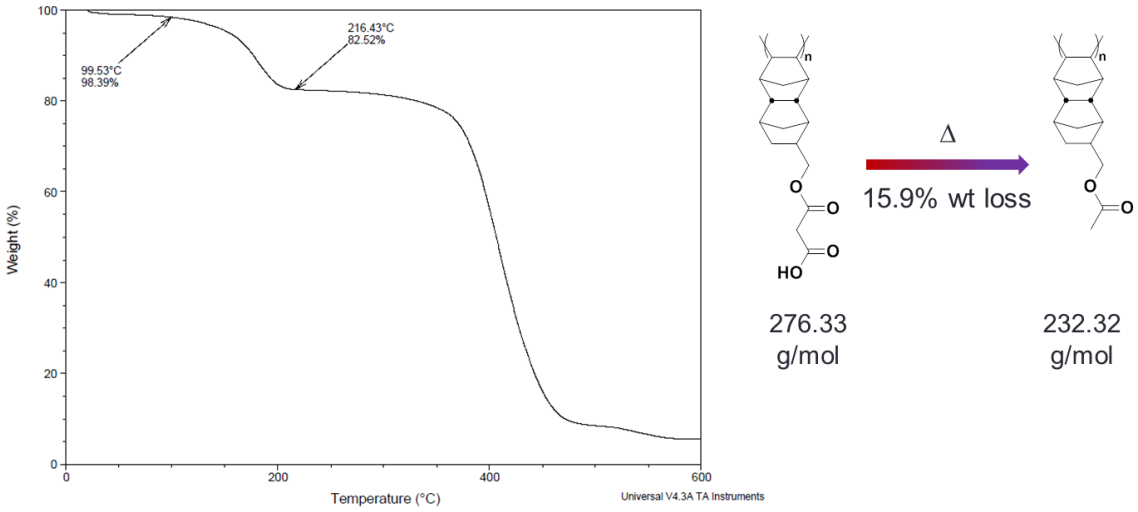

Figure 3.7. Thermal gravimetric analysis of the target polymer.

A goniometer was used to conduct a contact angle study with the polymer at the given stages in its process to compare the changes in molecular interactions with water, which are suggestive of the changes in surface energy (Figure 3.8).

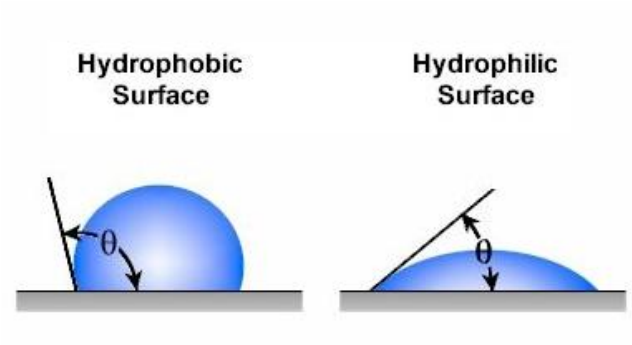

Figure 3.8. A larger contact angle of water with the substrate corresponds to a less polar compound. A smaller contact angle of water with the substrate corresponds to a more polar compound[34].

As seen in Figure 3.9, the contact angle of the polymer decreases as the tert-butyl ester is deprotected to the acid and converted to the salt, indicative of a significant polarity change. The contact angle of the conjugate base of the carboxylic acid is noticeably lower than the other materials, although sorption of the water droplet made measurements difficult. As expected, upon decarboxylation, the contact angle of the polymer increases, providing evidence of a polarity change to a less polar state.

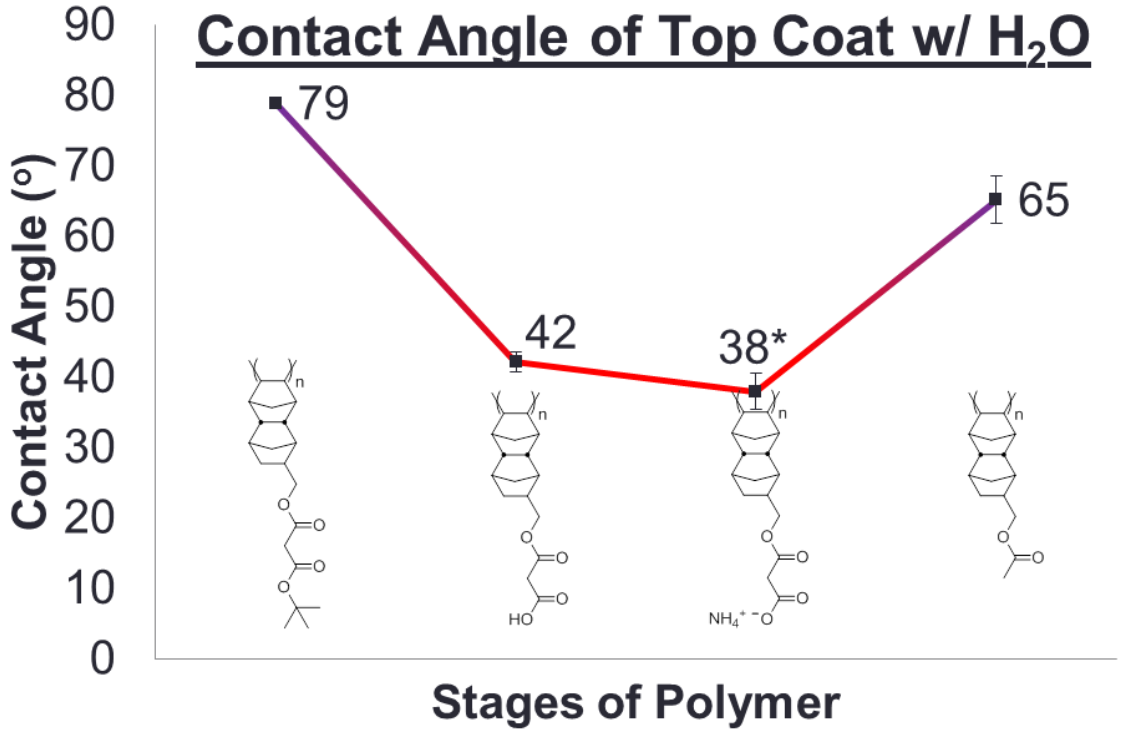

Figure 3.9. Contact angles of water droplets with the corresponding materials. *The salt form of the polymer gradually dissolved when in contact with water.

The polymer was applied as a topcoat over a BCP following the procedure outlined in Figure 3.1. The sample was heated at 200 ºC for 15 minutes to decarboxylate the top coat, causing the film thickness to decrease quickly, within the first minute, before stabilizing. The sample was then annealed for 17 hours in a vacuum oven at 170 ºC and was subjected to reactive oxygen ion etching to remove the top coat. Scanning

electron microscopy was used to visualize the post-anneal BCP, but perpendicular orientation was not observed, suggesting too large of a surface energy mismatch.

As discussed previously, the monomers **11** and **19** were not successfully polymerized using nickel-based catalysts. Collaborators Hugh Burgoon and Larry Rhodes of Promerus, LLC have conducted addition polymerization tests with the monomers shown in Figure 3.10 to determine the efficacy of polymerization using a cationic Group 10 metal complex and a weakly coordinating anion[35].

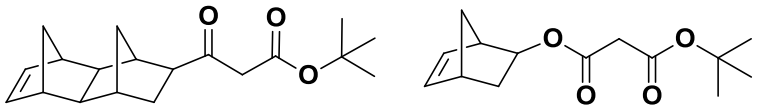

11 **19**

Figure 3.10. Monomers polymerized by Promerus, LLC.

Palladium(II) acetylacetonate was employed as the catalyst for the addition polymerization. Tricyclohexylphosphine and lithium tetrakis(pentafluoroborate) etherate were used as cocatalysts[35]. The reactions were run at 80 °C overnight in a 5 mL crimp cap vial equipped with magnetic stirring at a concentration of 1.2 M. The results of the polymerizations with different monomer/catalyst ratios are shown in Figure 3.11.

Exp	Monomer	Monomer:Pd:Cocatalysts	M_w (kDa)	PDI	% Conversion (GPC Area)
1	19	1000:1:2	131	3.6	34
2	11	1000:1:2	3	33.4	30
3	19	100:1:2	Insoluble	Insoluble	Insoluble
4	11	100:1:2	10	2.7	100
5	19	1000:1:2	23.2	1.9	34
6	11	1000:1:2	14.6	2.6	39
7	19	100:1:2 (with 30 % 1-hexene	Insoluble	Insoluble	Insoluble

Figure 3.11. Experimental results with varying monomer/catalyst loadings.

Polymers were obtained using the palladium catalyst but gave varying results. Experiments 1 and 5 should have produced the same results but gave inconsistent molecular weights and molecular weight distributions. Likewise, experiments 2 and 6, which should have produced the same results, were drastically different. In fact, experiment 3 yielded a product that was insoluble, presumably, due to high molecular weight despite having a lower monomer/catalyst loading. Experiment 7 included the addition of 1-hexene attempting to decrease molecular weights of the resulting polymers[35] but still produced an insoluble material. The experiments from Promerus, LLC. show the addition polymerization of norbornene-based monomers are possible using alternative catalysts, but the polymerizations are difficult to control. Due to the difficulty of the addition polymerization of β-keto acid containing norbornene compounds, other polymers with the β-keto acid functionality were pursued.

3.2. Ring Opening Metathesis Polymerization of Dinorbornene-Based Monomers for Decarboxylation

Grubbs' 2nd generation catalyst (G2) can generate polymers through the metathesis of olefin-containing, ring-strained monomers. Its appeal lies in its tolerance of multiple functional groups, air, and a wide range of solvents. This design is intended to enable the polymerization of the monomer with its β-keto ester functionality without requiring post-polymerization modification. However, the T_g's of metathesis polymers are typically too low to be applicable as a top coat for the Si-containing BCP. However, it was found that a metathesis polymer of the tetracyclic norbornene derivative, **1**, has a T_g over 200 °C (Figure 3.12).

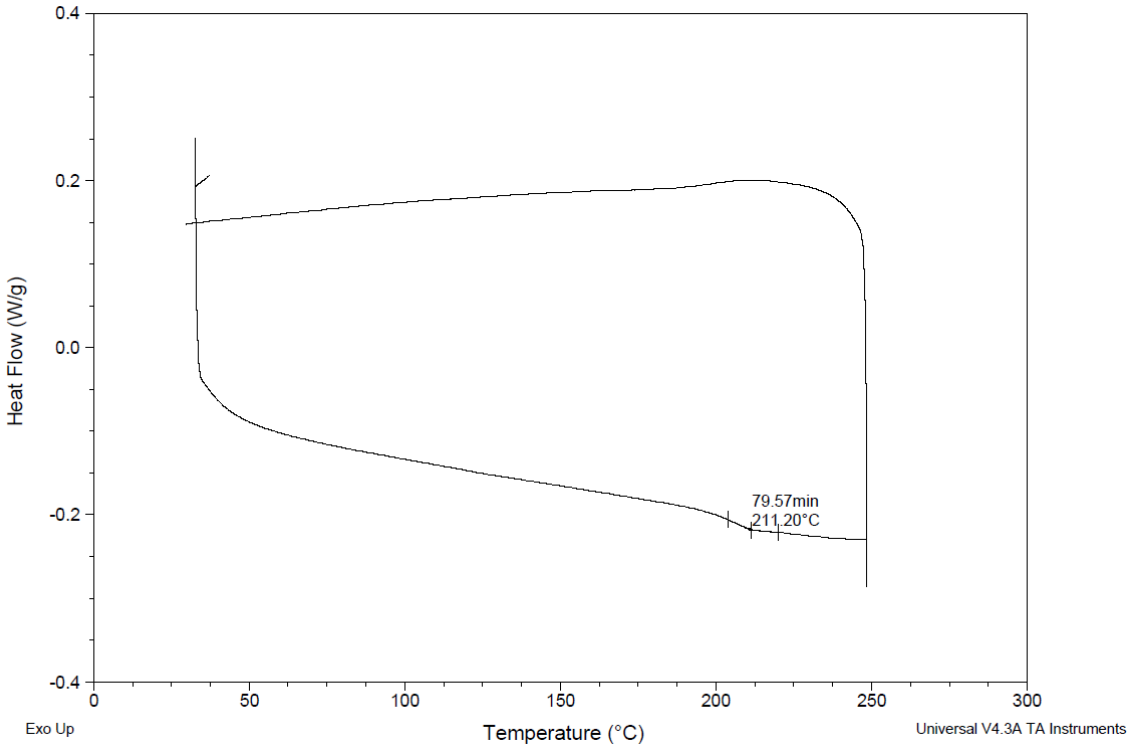

Figure 3.12. Differential scanning calorimetry trace of **1** showing a T_g of 211 °C

Confident in a high T_g polymer, **3** was reacted with G2 in tetrahydrofuran to obtain the metathesis polymer as shown in Figure 3.13. This polymerization proved to be difficult as gelation occurred at high concentrations. Ring opening metathesis polymerizations of tetracyclic norbornene derivatives with G2 were therefore conducted at low concentration.

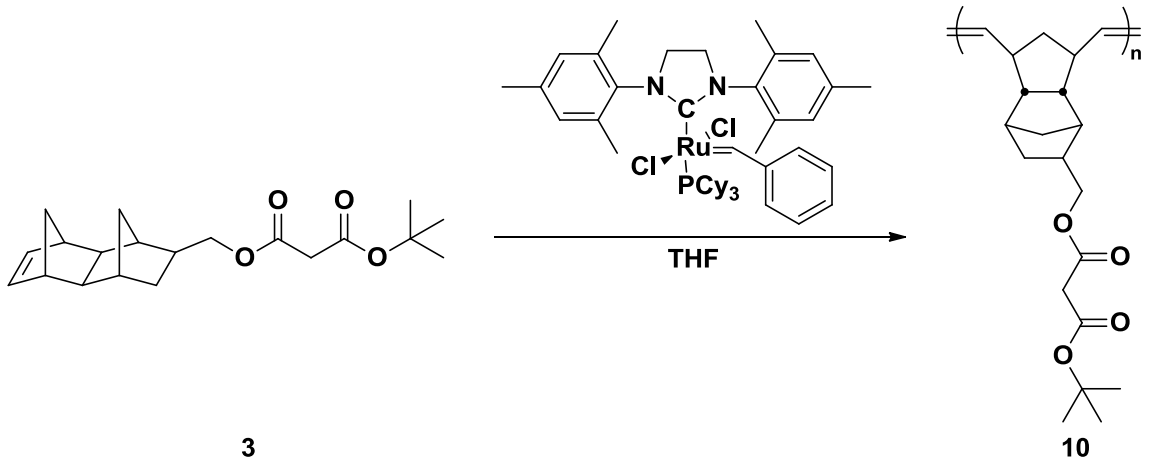

3 10

Figure 3.13. Metathesis polymerization of **3**.

A new cyclic norbornene monomer having the β-keto ester functionality without an acetate linkage was synthesized, in an attempt to improve its hydrolytic stability. Polymer **10** can eventually be hydrolyzed and result in the alcohol, thus its shelf-life was poor. In contrast, the deprotected version of **11** has no sites for hydrolysis (Figure 3.14). The polymerization concentration was optimized at 0.08 M as higher concentrations resulted in gelled reaction mixtures. It must be noted that the polymerization should be terminated and the product precipitated within three hours to avoid issues with gelation. Following deprotection using trifluoroacetic acid in methylene chloride, target polymer **13** was obtained. Unfortunately, the polymer was soluble in neither aqueous ammonium hydroxide nor mixtures with co-solvents methanol and isopropanol. **13** was also insoluble in an aqueous solution of trimethylamine. As stated previously, the conversion of the t-butyl ester to the carboxylic acid is very sensitive and is addressed in the following section. This may be attributed to the poor solubility characteristics of the polymer as the decarboxylation may have already occurred in some repeating units.

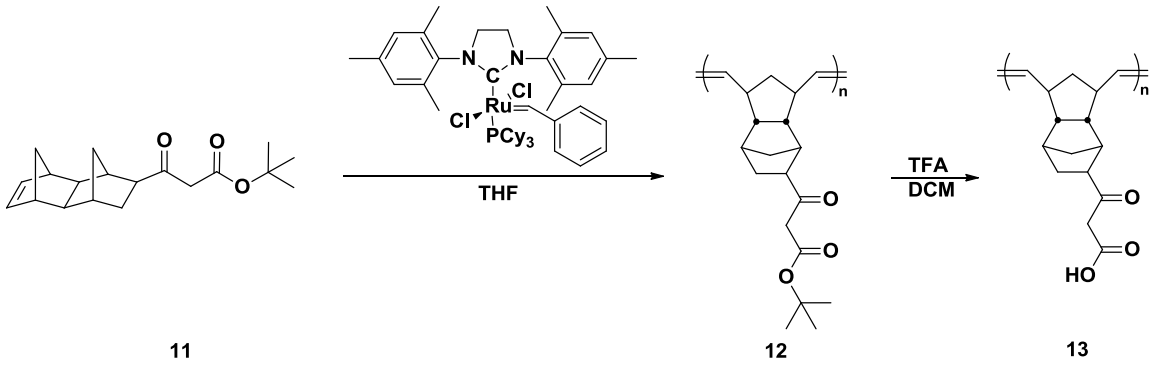

Figure 3.14. Metathesis polymerization of **11** followed by deprotection to yield homopolymer **13**.

Homopolymer **13** was analyzed by thermal gravimetric analysis to determine the temperature at which the decarboxylation would occur (Figure 3.15). The polymer exhibited a weight loss of about 18% upon heating, which corresponds to the decarboxylation, beginning at 100 °C and ending at 200 °C. No decomposition was observed following decarboxylation until 400 °C.

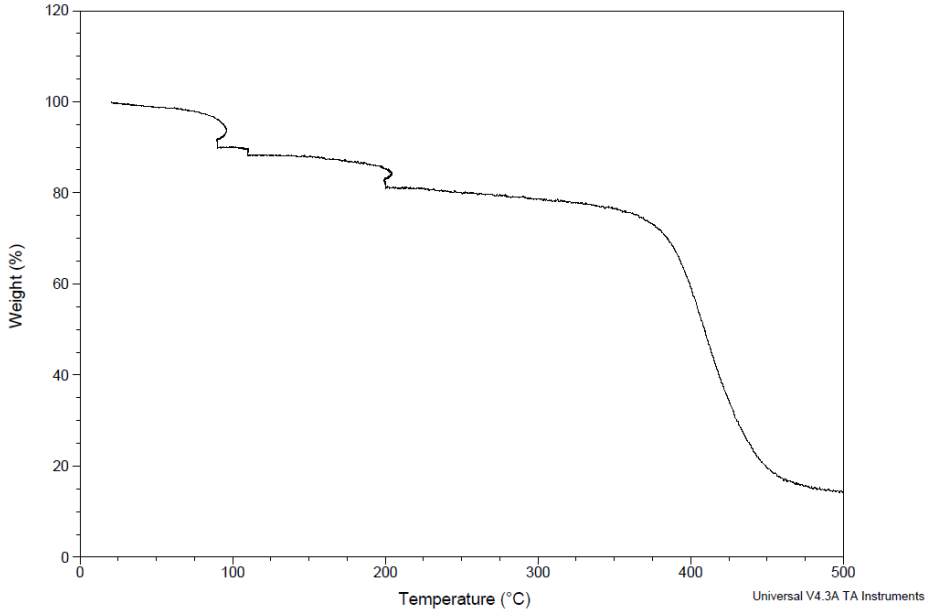

Figure 3.15. Thermal gravimetric analysis of **13**. The peculiar behavior at 100 °C, 110 °C, and 200 °C is attributed to modest overshoots in temperature during their isotherms.

With this promising result, **13** was decarboxylated by heating the solid at 250 °C for 1 hour on the TGA. Decarboxylation was complete within the 25 minutes required to heat the sample to 250 °C (Figure 3.16).

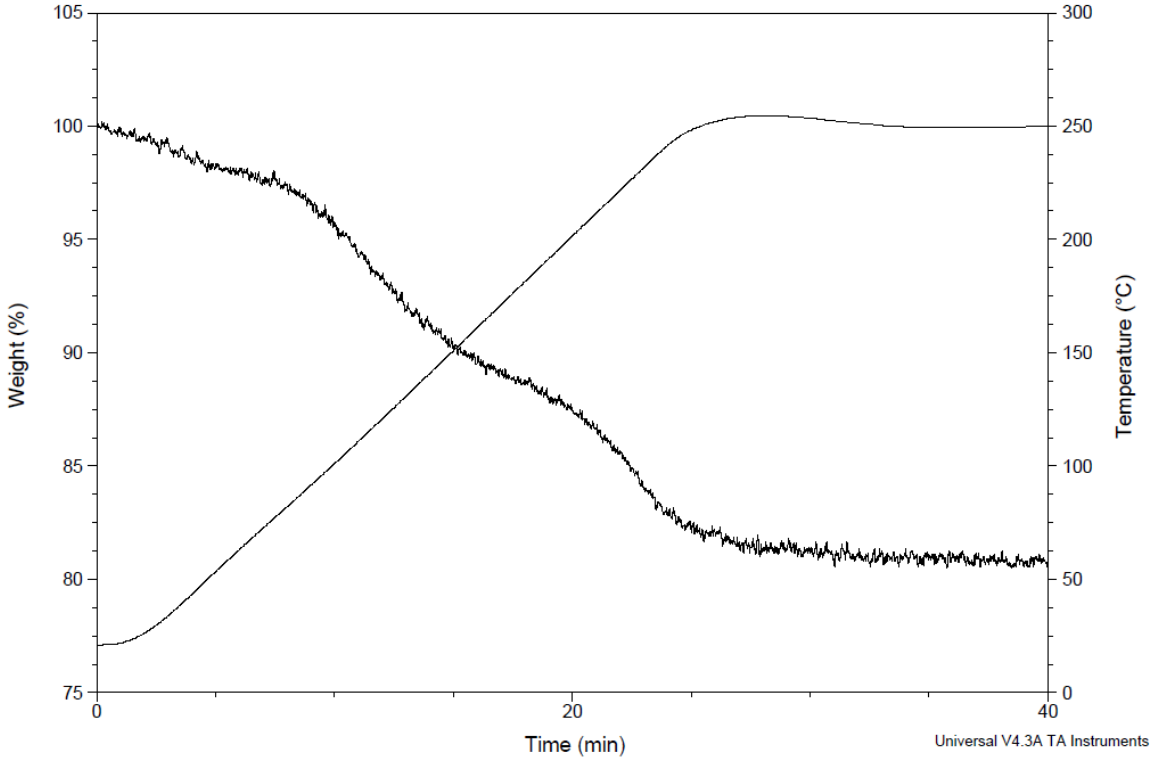

Figure 3.16. Thermal gravimetric analysis of the decarboxylation of **13**.

A sample of **13** was decarboxylated in the solid state, and differential scanning calorimetry was performed to find no observable T_g below 225 °C.

Using Grubbs' 2nd generation catalyst, a homopolymer of a tetracyclic norbornene derivative with β-keto acid functionality was synthesized. The polymer exhibited the desired characteristics of decarboxylation and high T_g. Unfortunately, the polymer was insoluble in aqueous base, which is required for application as a top coat to the non-aqueous soluble BCP.

3.3. Deprotection and Isolation of the β-Keto Acid

The isolation of the β-keto acid was a difficult task. Converting the ester in the polymer to the acid using trifluoroacetic acid oftentimes resulted in decarboxylation and formation of the resulting ketone. The deprotection must be performed at 0 °C and with a slow addition of a dilute solution of trifluoroacetic acid. This enables the isolation of the carboxylic acid polymer. The longevity of the acid, however, is limited (Figure 3.17).

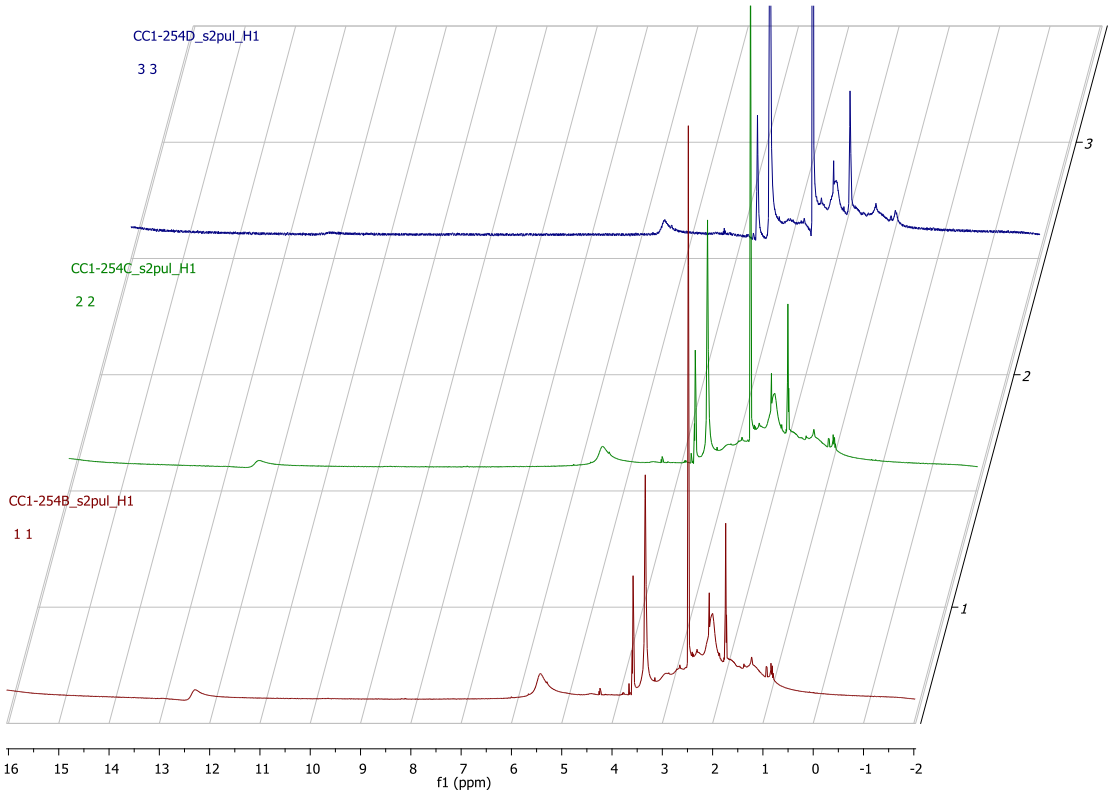

Figure 3.17. ^{1}H-NMR spectra showing the stability of the β-keto acid polymer, **13**, in deuterated DMSO. CC1-254D was taken 54 hours after the acid was first isolated.

The carboxylic acid peak at 12.4 ppm is no longer present after 54 hours of being in solution. This sensitivity to the deprotection of the t-butyl ester is unique to the polymer.

Subsequently, studies were conducted with monomeric materials to test the stability of β-keto esters and β-keto acids.

The carboxylic acid derivative of tetracyclododecene, **14**, was synthesized from the commercially available methyl ester derivative, **1**. **14** was used as a standard to compare the IR and NMR spectra of synthesized carboxylic acids (Figure 3.18).

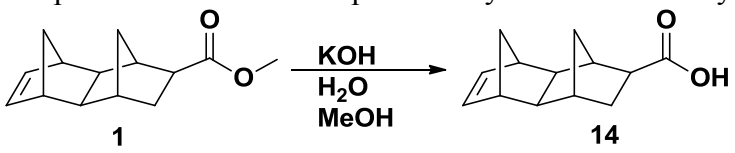

Figure 3.18. Synthesis of the tetracyclododecene carboxylic acid derivative, **14**.

The conversion of the ester to the corresponding carboxylic acid in the polymer often resulted in decarboxylation. The first small molecule study was conducted on the corresponding monomer, **11**, to see if the behavior was specific for the polymer (Figure 3.19).

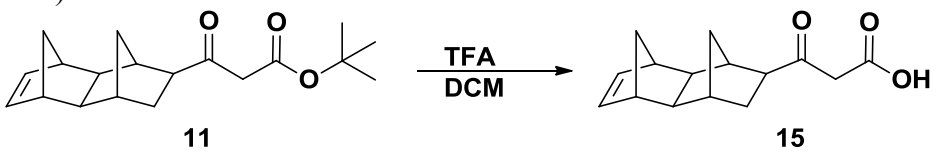

Figure 3.19. Conversion of the β-keto ester, **11**, to the β-keto acid, **15**.

The deprotection was conducted at room temperature with a high concentration of trifluoroacetic acid. The polymer, however, was deprotected at 0 ºC using a slow addition of dilute trifluoroacetic acid. In the small molecule, the carboxylic acid was isolated in high yield with no evidence by NMR of decarboxylation to the corresponding ketone. This further suggests the instability of the β-keto acid to be unique to the polymer.

Another issue encountered when conducting the polymerization of **11** was the need for immediate isolation of the polymer following the quenching of the

polymerization. The polymer of **11** can be precipitated in methanol immediately after the reaction. If the polymer is left in solution for over 4 hours following the reaction, it will no longer precipitate in methanol but in hexanes instead. For this reason, studies were conducted with G2 to see if it could convert the ester to the carboxylic acid. The monomer **11** was first hydrogenated to avoid polymerization in the presence of G2 (Figure 3.20).

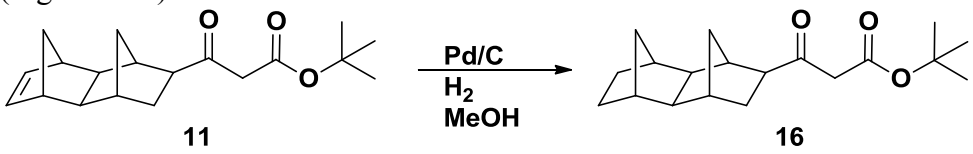

11 **16**

Figure 3.20. Hydrogenation of the β-keto ester monomer, **11**.

The hydrogenation was conducted successfully under mild conditions; the reaction proceeded at ambient temperature and 1 atm of hydrogen. The ketone and ester were left unaffected during the reduction of the alkene. NMR studies of G2 with **11** and with **16** were conducted in parallel. In separate NMR tubes, the structures of **11** and **16** were monitored in the presence of G2 over a period of 7 days. There was no observable change in the t-butyl ester peak in either sample during that time aside from the polymerization of **11**. The stability of the compounds in vacuum was tested by concentrating the samples in vacuo and redissolving them in deuterated chloroform. The structures of the compounds were unaffected when subjected to vacuum at a pressure of 0.6 torr. The β-keto esters in the polymer and monomer are stable in the presence of G2. No conversion to the carboxylic acid was detected. After confirming the stability of the β-keto ester functionality in both the monomer and polymer, experiments were conducted to test the stability of the acid.

The stability of the small molecule β-keto acid in solution was investigated with and without the presence of G2. The hydrogenated monomer, **16**, was deprotected in mild conditions to ensure the isolation of the carboxylic acid (Figure 3.21).

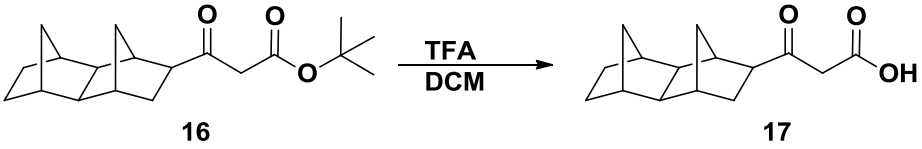

16 **17**

Figure 3.21. Synthesis of the β-keto acid, **17**. TFA was added slowly while at 0 ºC.

17 was immediately separated into two NMR tubes for monitoring structure changes: **17** in $CDCl_3$ (Figure 3.22) and **17** with G2 in $CDCl_3$ (Figure 3.23). The carboxylic acid was isolated, but the ketone peaks at 2.22 ppm and 2.20 ppm corresponding to decarboxylation were observed immediately. The following figures show the NMR spectra focused on the ketone region.

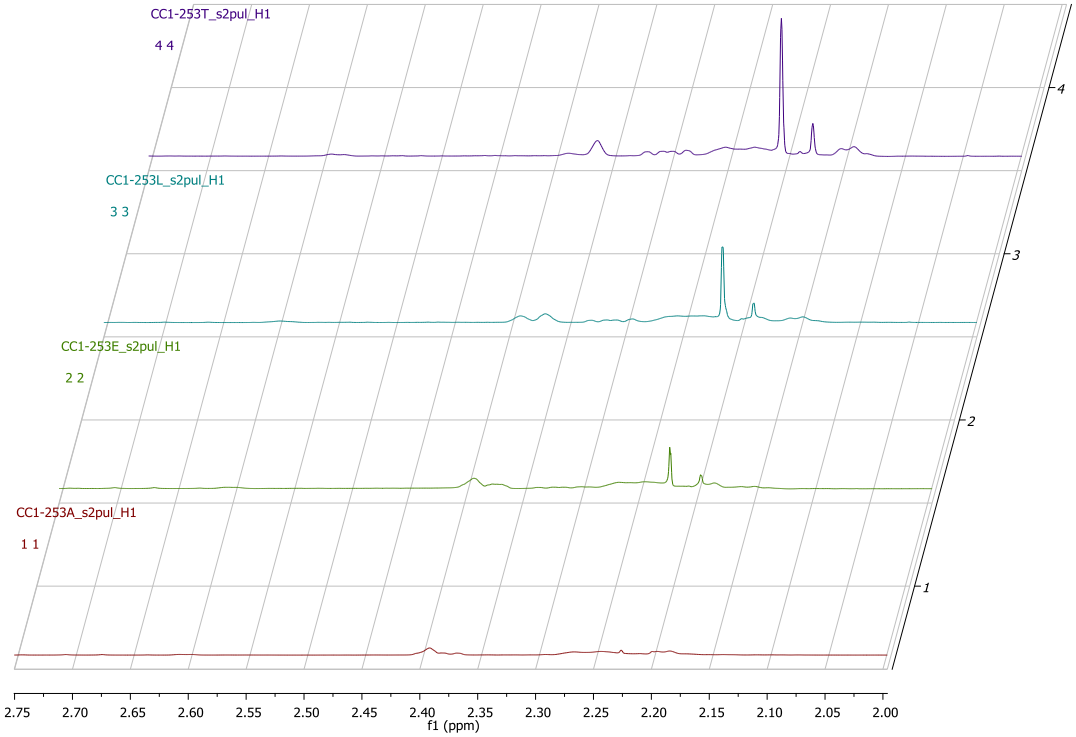

Figure 3.22. **17** in $CDCl_3$. The ketone peaks appear at 2.22 ppm and 2.20 ppm. The times for the spectra are as follows: A (0 hours), E (24 hours), L (74 hours), and T (198 hours).

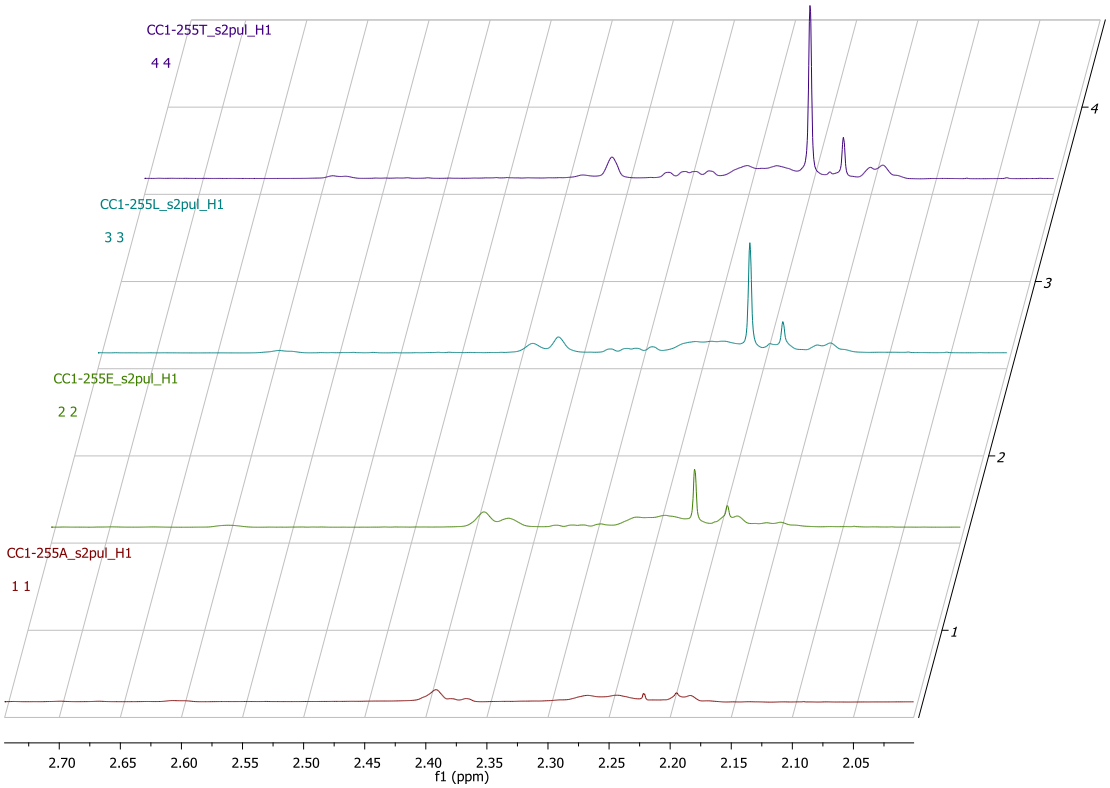

Figure 3.23. **17** and G2 in $CDCl_3$. The ketone peaks appear at 2.22 ppm and 2.20 ppm. The times for the spectra are as follows: A (0 hours), E (24 hours), L (74 hours), and T (198 hours).

The rate of decarboxylation is nearly identical for the two trials as G2 does not noticeably catalyze the reaction. After 200 hours, decarboxylation has occurred, but the carboxylic acid is still present. These results show the instability of the acid in the monomer in solution with no effects with the addition of G2, though decarboxylation occurs much more slowly than in the polymer.

The β-keto ester functionality is stable in both the monomer and polymer when in solution even in the presence of G2. The β-keto acid, however, has a limited lifetime in solution. When the polymer is in solution at ambient temperature, decarboxylation completes within 54 hours and the β-keto acid is fully converted into the corresponding

ketone. The small molecule maintains its β-keto acid functionality for much longer, though decarboxylation begins immediately. As the β-keto acid, the polymer has an extremely short shelf-life, which limits its potential application as a top coat.

3.4. SOLUBILITY SWITCH VIA CYCLIC ANHYDRIDES

Due to the instability of the β-keto acid, other mechanisms for a polarity switch were explored. Maleic anhydride possesses a polarity switching ability as shown in Figure 3.24.

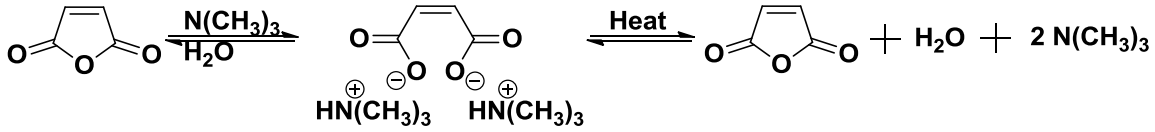

Figure 3.24. The reversible polarity switching mechanism of maleic anhydride

The anhydride can be dissolved in aqueous base, which causes it to open into the dicarboxylate salt. Upon heating, the dicarboxylate salt closes back into the less polar maleic anhydride, which modulates the surface energy[36]. Polymers containing maleic anhydride, however, are limited to alternating copolymers (Figure 3.25)[37].

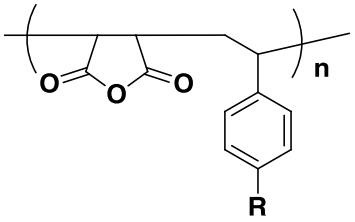

Figure 3.25. The alternating copolymer resulting from the polymerization of maleic anhydride and styrene derivatives.

This limits the compositional variance that can be achieved for the top coat materials, thus the surface energy spectrum may be limited. In the closed form, maleic anhydride is still relatively polar, and the copolymer may not possess a low enough surface energy to be employed as a top coat. In addition, the Tg of the top coat polymer is dependent on the

alternating structure, thus decoupling the polarity-switching mechanism from the attributes that give the polymer a large Tg would be advantageous.

The polarity switching mechanism of maleic anhydride can be found in a similar monomer, carbic anhydride. The anhydride moiety is attached to norbornene, enabling the monomer to be polymerized using G2 (Figure 3.26).

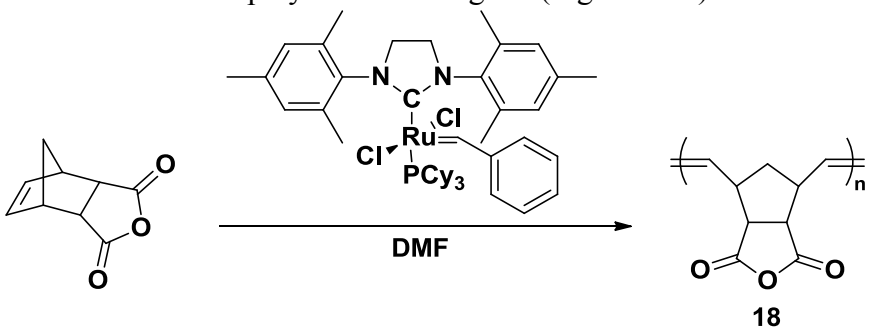

Figure 3.26. The homopolymerization of carbic anhydride with G2.

The homopolymer, **18**, did not exhibit a Tg prior to its decomposition temperature at 364 ^{o}C indicating its promise as a high Tg top coat material. The homopolymer, which is soluble in aqueous base, is too polar for a top coat on most block copolymers. However, using G2, carbic anhydride can be randomly copolymerized without limiting its composition in the polymer at 50 %.

To lower the surface energy of the carbic anhydride containing polymer, other monomers must be copolymerized. To maintain a high Tg, various tetracyclic dodecene based compounds were explored as comonomers. The comonomer candidates were homopolymerized with G2 to find their corresponding Tg's and Td's. These compounds were selected for their varying polarity with **20** as the most non polar and **22** as the most polar (Figure 3.27).

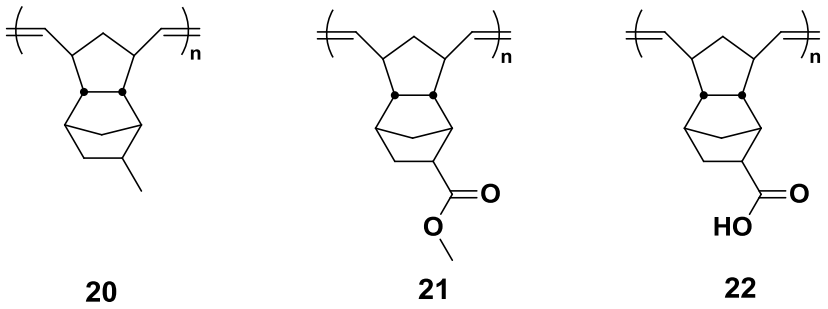

20 21 22

Figure 3.27. Structures of ring opening metathesis homopolymers to be copolymerized with carbic anhydride.

Homopolymer	**Tg (°C)**	**Td (°C)**
18	N/A	364
20	201	395
21	211	397
22	N/A	394

Figure 3.28. The temperatures for glass transition and decomposition of the homopolymers in Figure 3.27.

The polymers, **20** and **21**, exhibit Tg's over 200 °C, while all 4 homopolymers have Td's over 350 °C. With these high temperatures and **18** being readily soluble in aqueous base, metathesis copolymers containing **18** and varying amounts of **20**, **21**, or **22** may be synthesized for the potential application as top coat surface treatments.

3.5. FUTURE WORK

In summary, pathways to new types of top coat surface treatments have been established. The first class of polymers has β-keto acid functionality that produces a solubility switch via a decarboxylation mechanism. Both the ring opened metathesis polymer and addition polymer of the tetracyclic norbornene exhibit glass transition

temperatures well over that of the block copolymer which is advantageous for thermal annealing techniques. The metathesis polymer is a more attractive pathway as the only post-polymerization modification required is simple deprotection. Unfortunately, the deprotected β-keto acid containing polymers have short shelf-lives due to spontaneous decarboxylation at ambient temperatures. The second class of polymers relies on the anhydride functionality for a solubility switch. Initial tests with the homopolymers of carbic anhydride and tetracyclododecene monomers show high Tg's and Td's. Random copolymers can be synthesized with varying compositions of comonomers to vary the surface energy of the top coat polymers and be used for the orientation of BCP thin films.

Appendices

A1. OTHER NIARF CATALYST STUDIES

The NiArF catalyst reactivity scope was studied further. The dinorbornene methyl ester, **1**, was controllably polymerized to achieve targeted molecular weights and high yield when conducted in toluene. The polymerization of, **1**, was still successful when a stoichiometric amount of water-free ethyl acetate was added to the monomer. **1**, however, would not polymerize when tetrahydrofuran or ethyl acetate were used as the solvent. It is important to note that a 9:1 mixture of toluene and tetrahydrofuran can be used for an addition polymerization of a norbornene monomer with NiArF, if desired.

The dinorbornene alcohol from the reduction of the methyl ester could not be polymerized with NiArF. The dinorbornene carboxylic acid from the saponification of the methyl ester could not be polymerized with NiArF either. The lack of reaction was confirmed by ^{1}H-NMR.

A2. PROMERUS POLYMERIZATION RESULTS

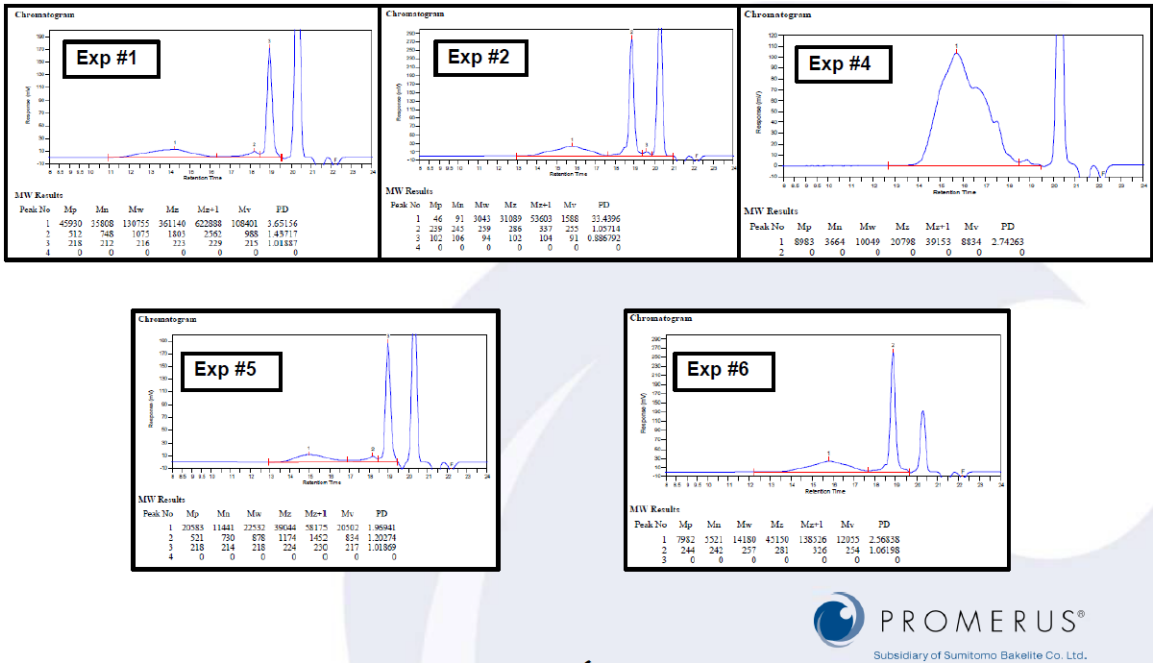

Figure A2.1. GPC traces of experiments.

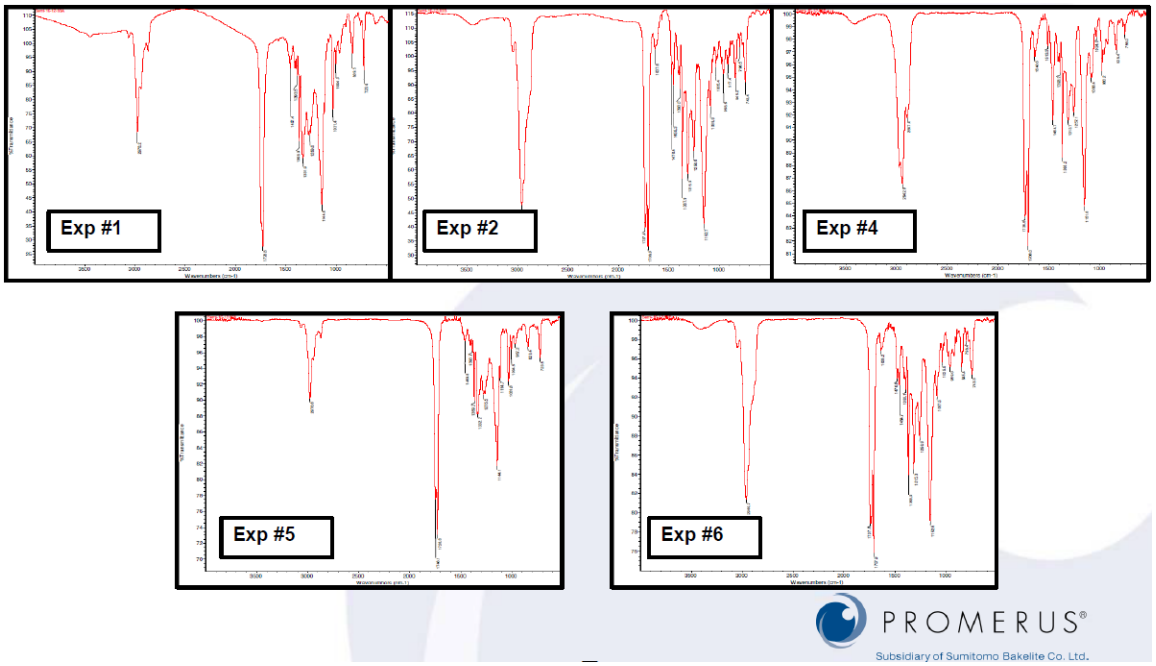

Figure A2.2. IR spectra of experiments. The t-butyl ester is unaffected by the polymerization conditions.

A3. EXPERIMENTAL PROCEDURES

General. Reagents were obtained from commercial sources and used without further purification unless specified otherwise. The tetracyclic norbornene methyl ester, **1**, used in derivation steps was obtained as a gift from *Japan Synthetic Rubber Co. Ltd.* The nickel catalyst (NiArF) used for addition polymerizations of norbornenes, (η^6-toluene)Ni(C_6F_5)$_2$, was obtained as a gift from *Promerus LLC*. The tetracyclic norbornene β-keto ester, **11**, was synthesized by Michael Maher. Methylene chloride (DCM) was dried by distillation over calcium hydride. Dry tetrahydrofuran (THF), dimethylformamide (DMF), and toluene were purified under argon through a solvent delivery system. Gel Permeation Chromatography (GPC) results were calculated using polystyrene standards. High Resolution Mass Spectrometry conducted with a Micromass Autospec Ultima. Nuclear magnetic resonance (NMR) spectra were obtained from a Varian Mercury 400 with VNMR 6.1C or a Varian DirectDrive 400 with VNMRJ 2.2C. Chemical shifts (∂) were reported in parts per million and referenced to the residual solvent peak.

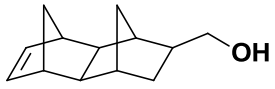

2

2. 400 mL dry THF was cannulated into a round bottom flask charged with lithium aluminum hydride (28g, 737 mmol) at 0 °C. The tetracyclic norbornene methyl ester, **1**, (66.008 g, 302.39 mmol) was dissolved in 50 mL dry THF and slowly added to the above heterogenous mixture. The mixture was then refluxed for 20 hours. It was then quenched sequentially with ice, water, and dilute hydrochloric acid. This mixture was allowed to stir overnight then extracted with DCM; the organic layer was washed with aqueous

ammonium chloride and brine, dried over magnesium sulfate, and condensed in vacuo to give a yellow oil. The crude mixture was purified by distillation (101-104 ºC, 0.60 Torr) to give an extremely viscous, colorless oil (55.814 g, 97%). ^{1}H-NMR (400 MHz, $CDCl_3$): 6.01 (m, 1H), 5.95 (m, 1H), 3.74 (t, 2H), 3.62 (m, 1H), 3.34 (m, 1H), 2.84 (b, 2H), 2.19 (2H), 2.00 (m, 2H), 1.85 (q, 2H), 1.65 (m, 1H), 1.50 (m, 1H), 0.61 (m, 1H), 0.45 (m, 1H). HRMS-CI (m/z): $[M+H]^+$ $C_{13}H_{18}O$ calcd. 191.1436, found 191.1436.

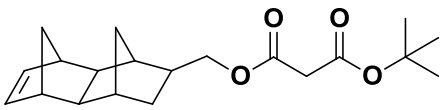

3

3. *N*-(3-dimethylaminopropyl)-*N'*-ethylcarbodiimide hydrochloride (1.303 g, 8.3934 mmol) and 4-dimethylaminopyridine (0.059 g, 0.4829 mmol) were added to a round bottom flask with a side arm. The reagents were left under high vacuum for 30 minutes, then 40 mL dry DMF added. The mixture was heated to dissolve the reagents, then cooled to 0 ºC, and tert-butyl hydrogen malonate (1.433 g, 8.9467 mmol) was syringed into the mixture. At this point, the colorless solution changed to a yellow color after stirring at 0 ºC for 10 minutes. After warming to ambient temperature, a solution of **2** in 10 mL dry DMF was added by syringe. The resulting mixture changed to a green color within 30 minutes. Seventeen hours later, 100 mL water was added and stirred for 30 minutes. After adding 150 mL diethyl ether to the mixture, the organic phase was separated and extracted with 5 x 50 mL water and 50 mL brine. The mixture was dried over magnesium sulfate and concentrated in vacuo to give a colorless oil (2.310 g). Column chromatography was performed with 5 % ethyl acetate in hexanes to give the product as a colorless oil (1.182 g, 47%). ^{1}H-NMR (400 MHz, $CDCl_3$): 6.01 (q, 1H), 5.93 (m, 3H), 3.62 (q, 2H), 3.33 (m, 4H), 2.83 (b, 4H), 2.19 (m, 3H), 2.01 (m 7H), 1.48 (s,

9H), 1.22 (m, 8H), 0.86 (m, 2H), 0.61 (q, 2H), 0.45 (m 1H). ^{13}C-NMR (400 MHz, $CDCl_3$): 172.5, 166.4, 83.3, 42.4, 28.3. HRMS-CI (m/z): $[M+H]^+$ $C_{20}H_{29}O_4$ calcd. 333.2066, found 333.2064.

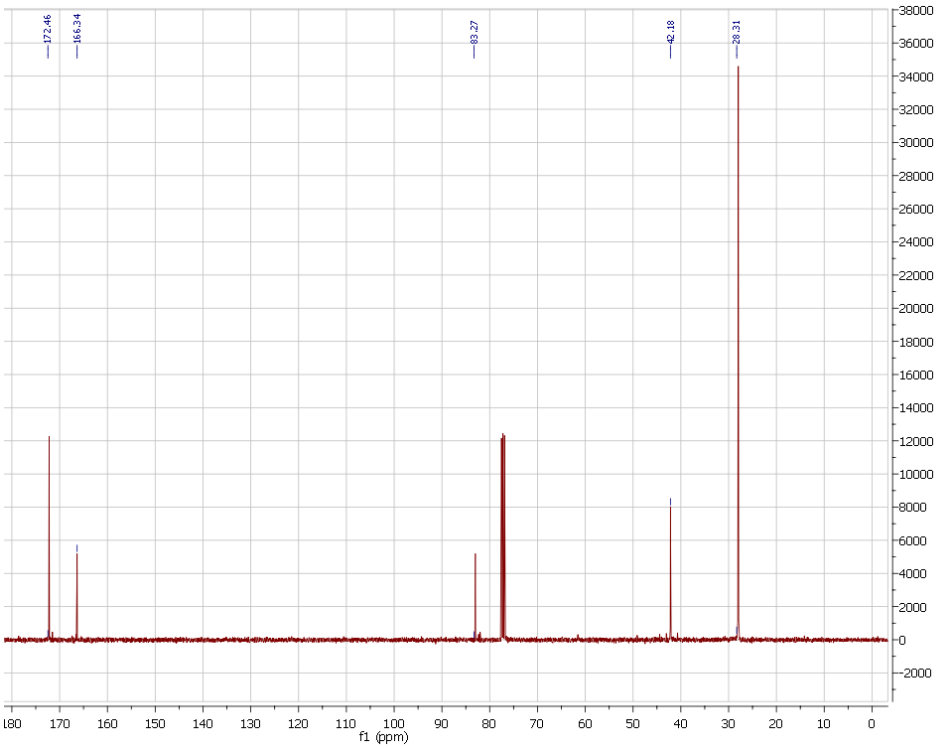

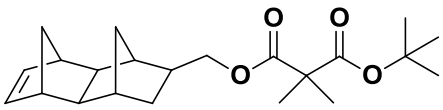

4

4. The malonate functionalized tetracyclic norbornene, **3**, (0.825 g, 2.481 mmol) was dissolved in 10 mL dry THF. Potassium tert-butoxide (0.597 g, 5.320 mmol) was added with a dry nitrogen purge, and the mixture turned yellow. Iodomethane (0.35 mL, 5.622 mmol) was distilled from calcium chloride in a Hickmann still and added dropwise to the previous mixture, which immediately generated an off-white precipitate. After 30 minutes, the precipitate was removed and an extraction was conducted on the solution

with aqueous ammonium chloride and brine. The organic layer was then dried over magnesium sulfate and condensed in vacuo to yield a colorless oil (0.572 g). Column chromatography at a 5% ethyl acetate/hexanes mixture resulted in the pure compound as a colorless oil (0.456 g, 51%). ^{1}H-NMR (400 MHz, $CDCl_3$): 5.99 (m, 1H), 5.93 (t, 3H), 4.1 (m, 3H), 3.84 (m, 3H), 3.48 (q, 1H), 2.83 (b, 5H), 2.16 (m, 4H), 2.02 (m, 4H), 1.95 (4H), 1.44 (s, 7H), 1.39 (s, 9H), 1.39 (m, 10H), 0.90 (q, 2H), 0.62 (d, 2H), 0.52 (m, 1H). HRMS-CI (m/z): [M] $C_{22}H_{32}O_4$ calcd. 360.2301, found 360.2301.

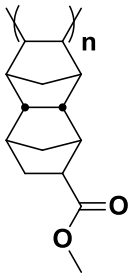

5

5. The tetracyclic norbornene methyl ester, **1**, was purified by distillation (73-77 ºC, 0.65 Torr) and kept under dry nitrogen. **1** (2.819 g, 12.914 mmol) was dissolved in 40 mL dry toluene under dry nitrogen. NiArF (.0628 g, 0.129 mmol) was added to a recovery flask in a drybox and dissolved in 3 mL dry toluene. The NiArF solution was added to the monomer solution at ambient temperature under dry nitrogen and stirred for 24 hours. The mixture was concentrated to about 10 mL toluene and added to 500 mL methanol. The off-white precipitate was isolated and dried (2.225 g, 78.9%). M_n = 58.5 kDa, M_w = 85.6 kDa, PDI = 1.5.

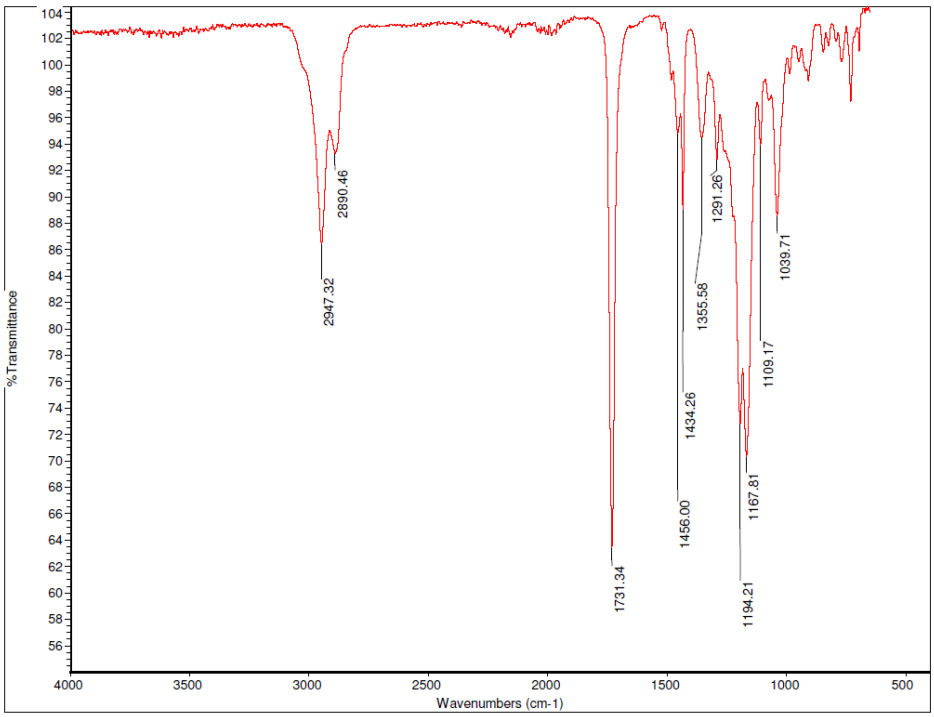

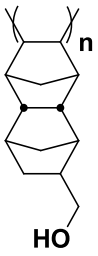

6

6. Dry THF (7.5 mL) was added to lithium aluminum hydride (0.580 g, 15.283 mmol) at 0 °C in dry glassware and under dry nitrogen. Homopolymer **5** was dissolved in 8 mL dry THF and added slowly by syringe into the LAH mixture. The reaction immediately increased in temperature, a solid appeared. To increase dissolution, 10 more mL dry THF was added and the reaction heated to 88 °C to break apart the solid. It was then cooled to 0 °C and quenched by pouring onto 300 mL of ice then hydrochloric acid added to yield an isolated white powder (0.651g, 73%).

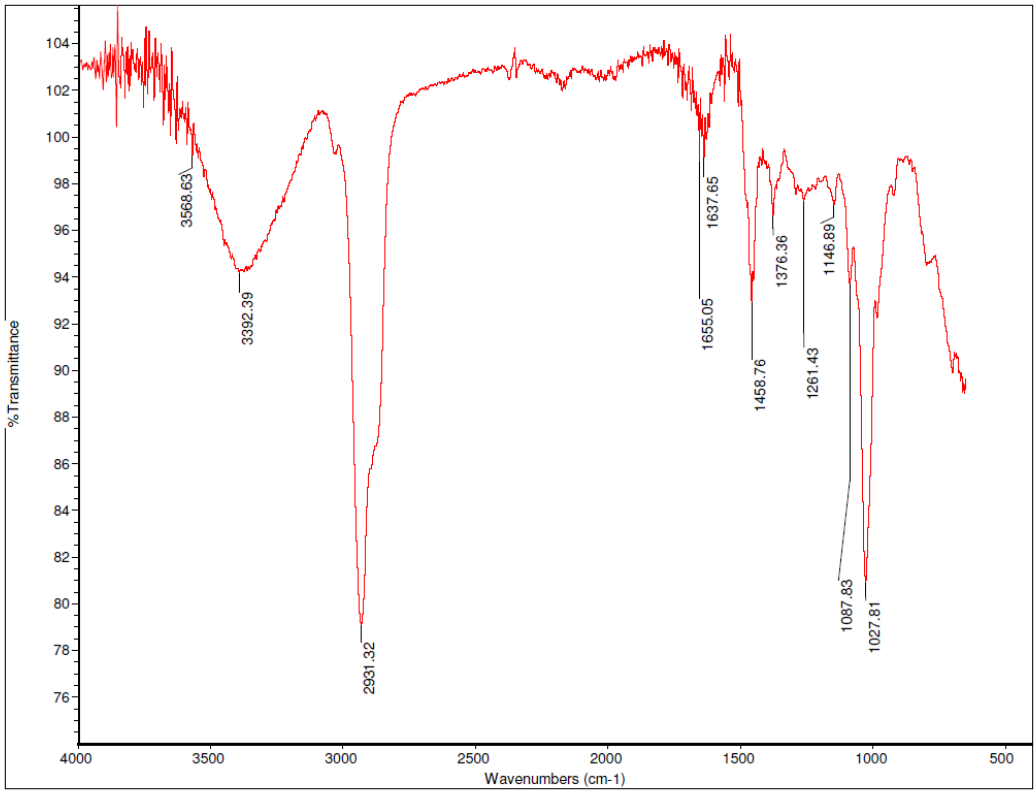

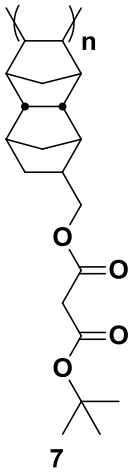

7

7. The alcohol functionalized homopolymer **6** (0.283 g, 1.487 mmol) was dried on high vacuum and dissolved in 17 mL dry DMF. The dissolution required vigorous stirring but was complete in 15 minutes. At 0 °C, tert-butyl hydrogen malonate (0.26 mL, 1.688

mmol), EDC (0.385 g, 2.008 mmol), and DMAP (0.018 g, 0.147 mmol) were added. The reagents were fully dissolved upon warming to ambient temperature at which point the solution became a light yellow color. After 18 hours, the functionalization was completed as confirmed by IR. The mixture was added to methanol and yielded a white precipitate. Upon isolation and drying, the product was obtained as a white solid (0.286 g, 58%).

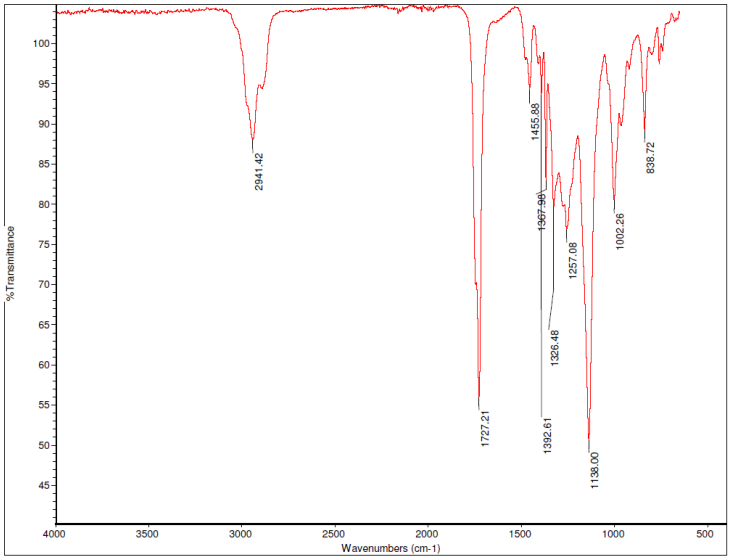

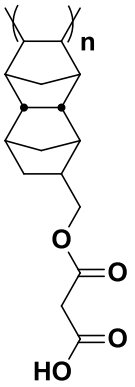

8

8. The malonate functionalized homopolymer **7** (0.251 g, 0.755 mmol) was dissolved in 6 mL DCM, which resulted in a green color in the solution. Trifluoroacetic acid (1.5 mL) was added and changed the solution color to red. After 1.5 hours, the mixture was

concentrated by charging air over the top of the stirring mixture. To ensure complete loss of trifluoroacetic acid, the polymer was redissolved in DCM, concentrated with an air purge, redissolved in THF, concentrated with an air purge, redissolved in THF, and precipitated into hexanes. The product **8** was isolated and dried to yield a white solid (0.141 g, 68%). After decarboxylation by heating, differential scanning calorimetry exhibited no observable T_g below 225 ºC.

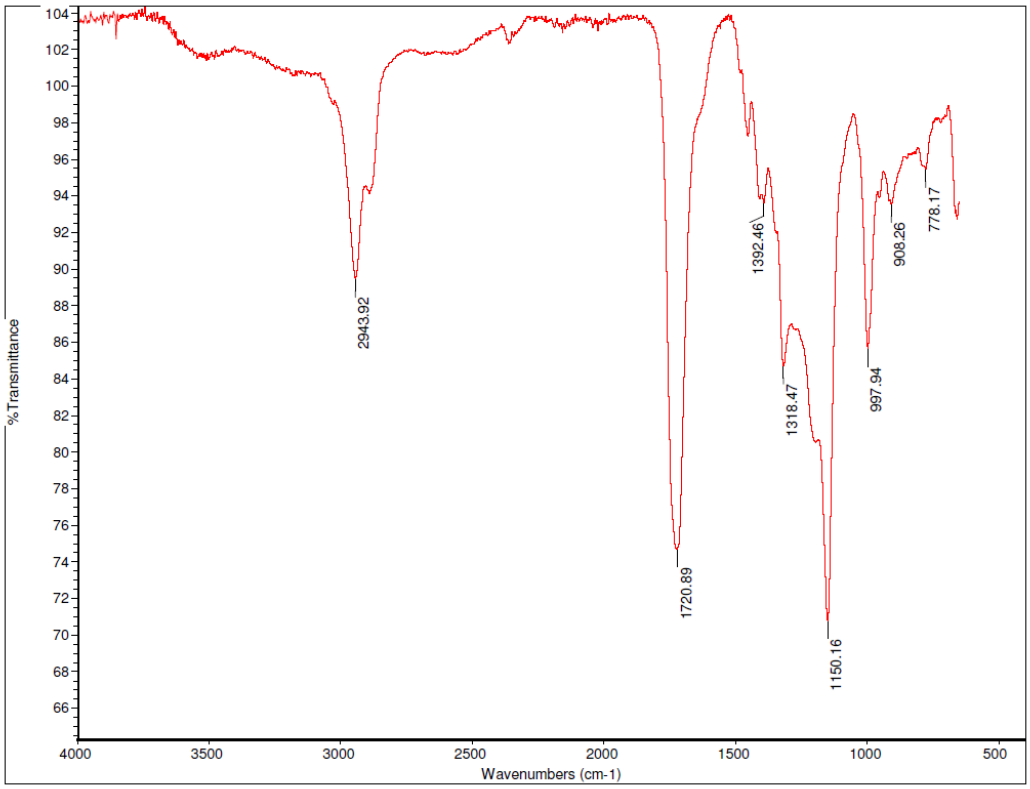

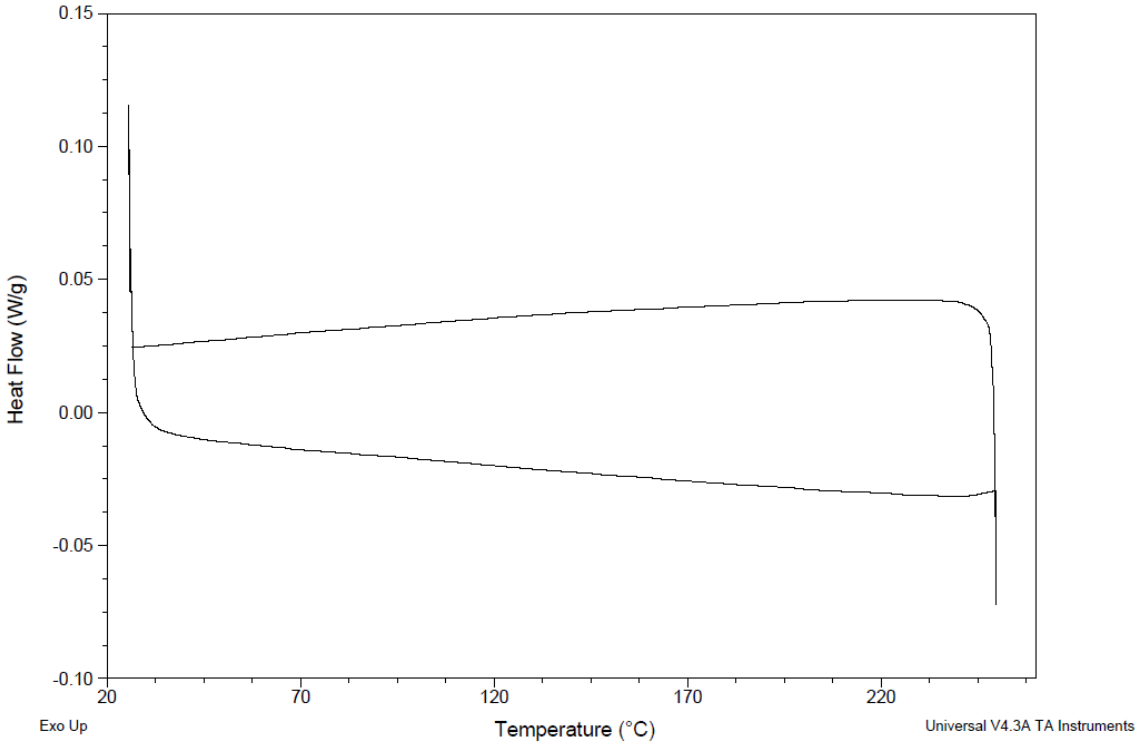

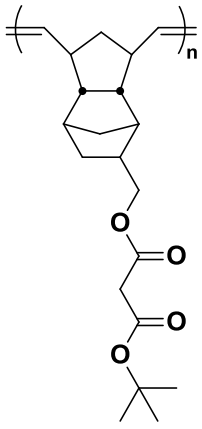

10

10. The tetracyclic malonate functionalized norbornene **3** (0.558 g, 1.678 mmol) was dissolved in 10 mL dry THF under dry nitrogen. G2 (0.015 g, 0.0176 mmol) was added to the monomer solution under positive dry nitrogen pressure. Gelation was observed within 30 minutes, so 10 mL dry THF was added to solubilize the polymer. After full

dissolution (3 hours), 3 mL ethyl vinyl ether was added. The mixture was precipitated into methanol but left a precipitate too fine to be isolated by filtration. The mixture was centrifuged, decanted, and solid dried on high vacuum. The resulting solid, however, was insoluble in DCM, THF, chloroform, acetone, toluene, DMF, and DMSO. No yield was obtained.

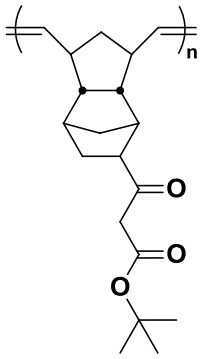

12

12. The tetracyclic β-keto ester functionalized norbornene **11** was synthesized and purified by Michael Maher. The monomer (0.940 g, 3.108 mmol) was dried on high vacuum, then dissolved in 40 mL dry THF. G2 was added to the monomer solution, and the solution changed to a dark brown color. After 16 hours, 7 mL ethyl vinyl ether was added to quench the reaction. At the same concentration, the mixture was then precipitated into 400 mL methanol. Filtration and drying of the precipitate gave an off-white solid (0.775 g, 82%).

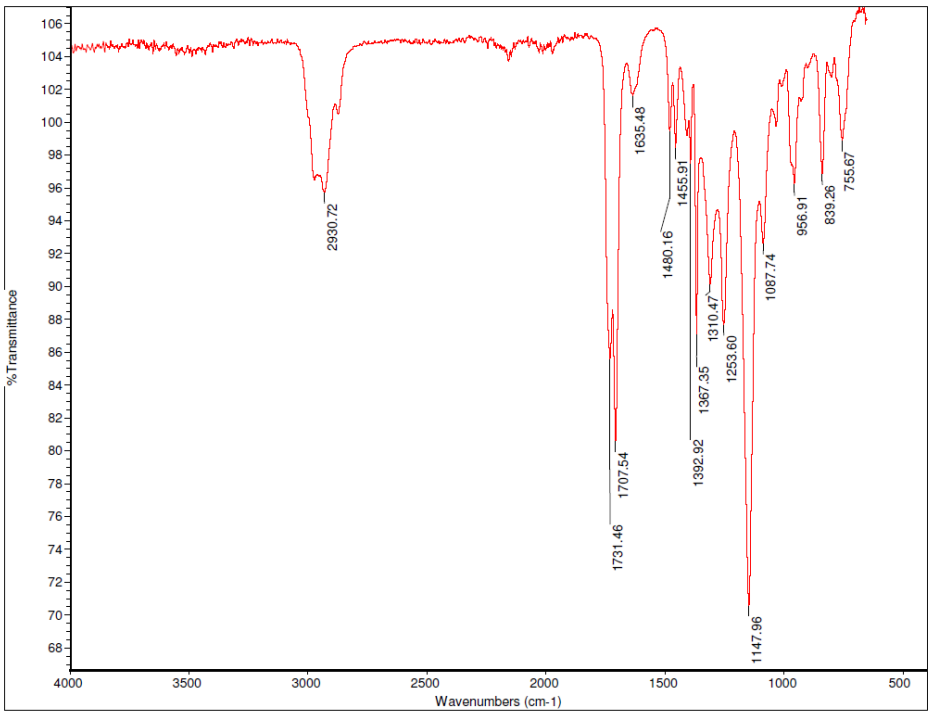

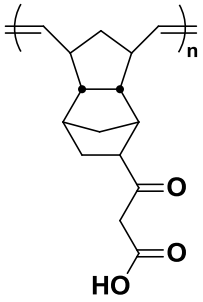

13

13. The protected homopolymer **12** (0.108 g, 0.357 mmol) was dissolved in 4 mL DCM, which turned the solution light orange. The solution was cooled to 0 °C, and 1 mL TFA was added dropwise. The first drop of TFA changed the solution color to yellow but eventually became black as the remainder of the 1 mL TFA was added. After 1.5 hours, the solution had become a dark blue. After concentrating the polymer with an air purge, the polymer was redissolved in THF and precipitated into hexanes. Filtration and drying

of the precipitate isolated an off-white solid (0.055g, 76%). The existence of the carboxylic acid was confirmed by IR and ^{1}H-NMR. After decarboxylation via heating, differential scanning calorimetry exhibited no observable T_g below 225 ^{o}C.

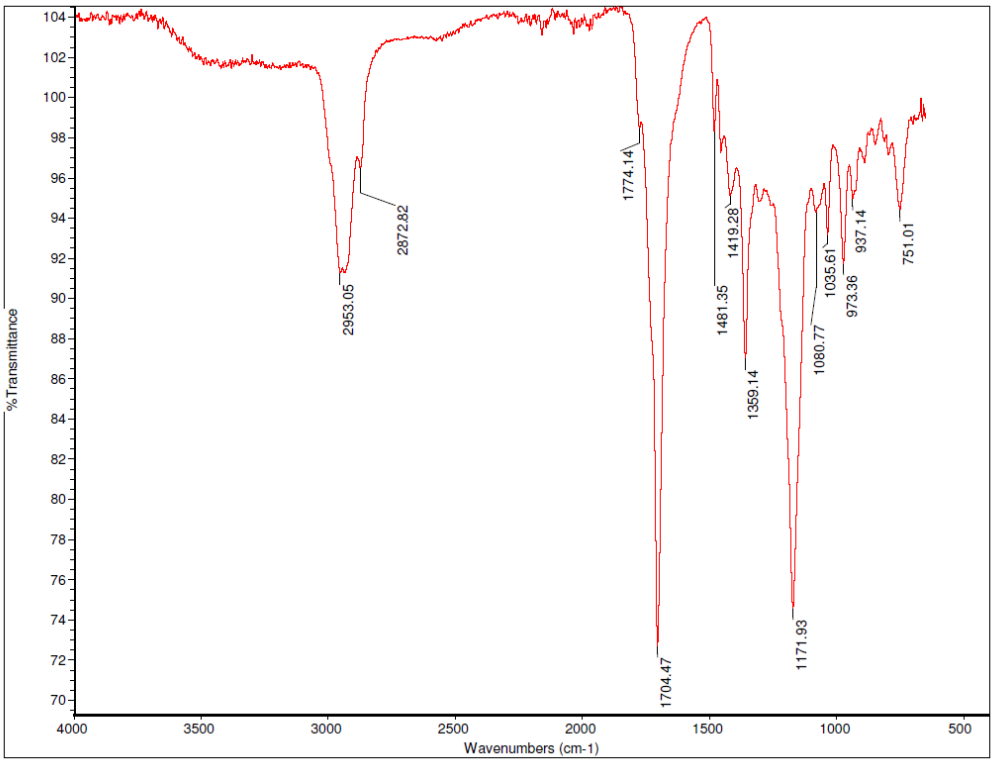

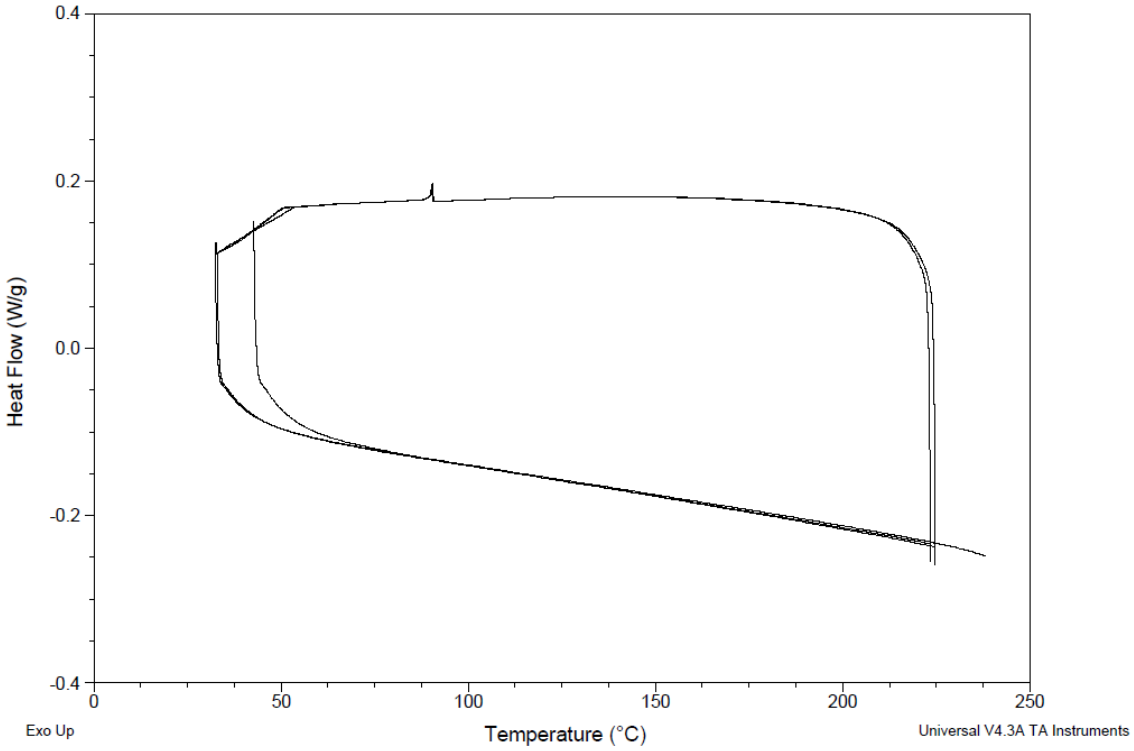

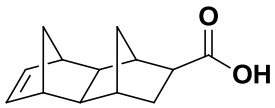

14

14. The methyl ester functionalized tetracyclic dodecene, **1**, (22.824 g, 104.558 mmol) and potassium hydroxide (10.307 g, 183.707 mmol) were dissolved in 250 mL water and 250 mL methanol. The reaction mixture was stirred at ambient temperature for 14 hours. Dilute hydrochloric acid was slowly added until the solution was strongly acid and white precipitate formed. The carboxylic acid was isolated as a white precipitate (19.361 g, 91%). ^{1}H-NMR (400 MHz, $CDCl_3$): 11.68 (b, 1H), 5.95 (m, 2H), 2.86 (b, 2H), 2.64 (m, 0.5H), 2.47 (m, 0.5H), 2.42 (s, 0.5H), 2.25 (m, 0.5H), 2.19 (m, 0.5H), 2.06 (m, 3.5H), 1.77 (m, 0.5H), 1.62 (m, 0.5H), 1.45 (m, 0.5H), 1.31 (m, 1.5H), 1.16 (m, 1H), 0.78 (d,

0.5H), 0.69 (m, 0.5H). HRMS-ESI (m/z): $[M-H]^-$ $C_{13}H_{16}O_2$ calcd. 203.10780, found 203.10780.

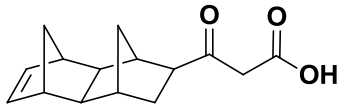

15

15. The tetracyclic β-keto ester functionalized norbornene **11** (1.108 g, 3.664 mmol) was dissolved in 3 mL dry dichloromethane. 3 mL trifluoroacetic acid was added, and the resulting mixture was stirred for 2 hours under dry nitrogen. The mixture was concentrated under nitrogen into an orange oil. ^{1}H-NMR (400 MHz, $CDCl_3$): 9.08 (bs, 4H), 5.09 (m, 1H), 4.72 (d, 1H), 4.58 (s, 1H), 3.62 (m, 2H), 3.48 (bs, 1H), 2.78 (t, 1H), 2.65 (t, 1H), 2.48 (m, 3H), 2.32 (m, 3H), 1.92 (m, 2H), 1.80 (m, 2H), 1.46 (d, 2H), 1.34 (m, 3H), 0.98 (m, 1H).

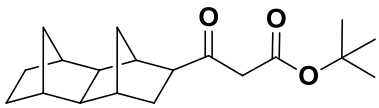

16

16. The tetracyclic β-keto ester functionalized norbornene **11** (0.780 g, 2.579 mmol) was dissolved in dry methanol. 5 % palladium on carbon (0.118 g) was added to the solution. The mixture was purged with hydrogen for 30 minutes and stirred at ambient temperature

under 1 atm of hydrogen for 15 hours. The reaction mixture was filtered through celite and a 0.2 μm PTFE filter. The solution was concentrated in vacuo to yield the colorless oil (0.744 g, 95 %). ^{1}H-NMR (400 MHz, $CDCl_3$): 3.36 (s, 1H), 2.37 (m, 1H), 2.21 (bs, 2H), 2.14 (d, 1H), 1.88 (q, 1H), 1.71 (s, 1H), 1.54 (d, 1H), 1.44 (s, 8H), 1.29 (d, 2H), 1.19 (m, 2H), 0.99 (d, 1H). HRMS-ESI (m/z): $[M+Na]^+$ $C_{19}H_{28}O_3$ calcd. 327.19310, found 327.19340.

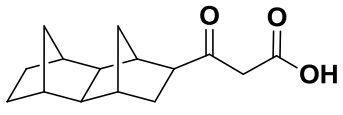

17

17. The hydrogenated tetracyclic β-keto ester, **16**, (0.209 g, 0.686 mmol) was dissolved in 3 mL dry dichloromethane. At 0 ^{o}C, 2 mL trifluoroacetic acid was added to the solution and stirred for 15 minutes. The mixture was then allowed to gradually warm to ambient temperature and stirred for an additional hour. The compound was concentrated under nitrogen to yield a colorless oil. ^{1}H-NMR (400 MHz, $CDCl_3$): 10.86 (sb, 2H), 3.61 (q, 2H), 2.89 (q, 1H), 2.76 (d, 1H), 2.69 (d, 1H), 2.58 (s, 1H), 2.38 (s, 2H), 2.23 (m, 4H), 1.88 (m, 1H), 1.72 (s, 2H), 1.56 (d, 2H), 1.42 (d, 3H), 1.29 (m, 3H), 1.18 (m, 2H), 1.00 (d, 1H).

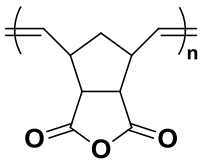

18

18. Carbic anhydride (0.504 g, 3.0702 mmol) was dissolved in 3 mL dry dimethylformamide (DMF). G2 (0.013 g, 0.0153 mmol) was dissolved in 3 mL dry DMF. The G2 solution was added into the carbic anhydride solution at 0 ^{o}C and stirred. After 30 minutes, the mixture was removed from the ice bath and allowed to warm to ambient temperature. After another 30 minutes, the mixture was slowly added to ethyl acetate to precipitate the polymer. The polymer was filtered and dried on high vacuum to yield a white solid (0.352 g, 70 %). M_n = 28 kDa, M_w = 52 kDa, PDI = 1.8.

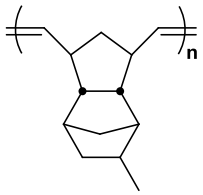

20

20. Methyl tetracyclododecene (2.243 g, 12.870 mmol) was dissolved in 110 mL toluene. G2 (0.036 g, 0.042 mmol) was dissolved in 2 mL toluene and added to the monomer solution. After stirring for 2 hours at ambient temperature, 6 mL ethyl vinyl ether was added to quench the polymerization. The mixture was poured into methanol to precipitate

the polymer. The polymer was filtered and dried on high vacuum to yield a grey solid (2.076 g, 93 %). M_n = 54 kDa, M_w = 78 kDa, PDI = 1.4.

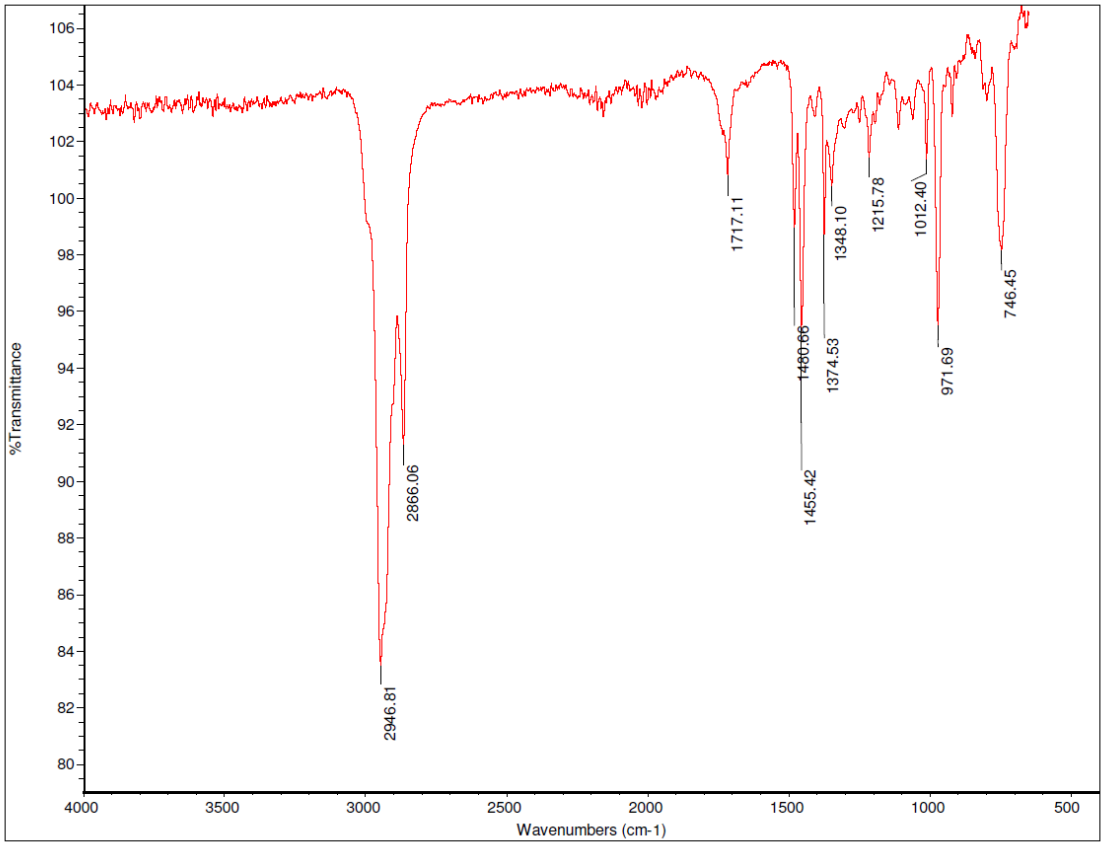

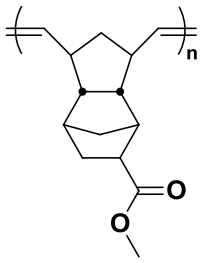

21

21. The methyl ester functionalized tetracyclododecene, **1**, (0.580 g, 2.657 mmol) was dissolved in 46 mL dry tetrahydrofuran (THF). G2 was dissolved in 2 mL dry THF and added to the monomer solution. After stirring for 1 hour 25 minutes, 4 mL ethyl vinyl ether was added. The mixture was poured into methanol to precipitate the polymer. The polymer was filtered and dried on high vacuum to yield a white solid (0.546 g, 94 %). M_n = 19.4 kDa, M_w = 23.2 kDa, PDI = 1.2.

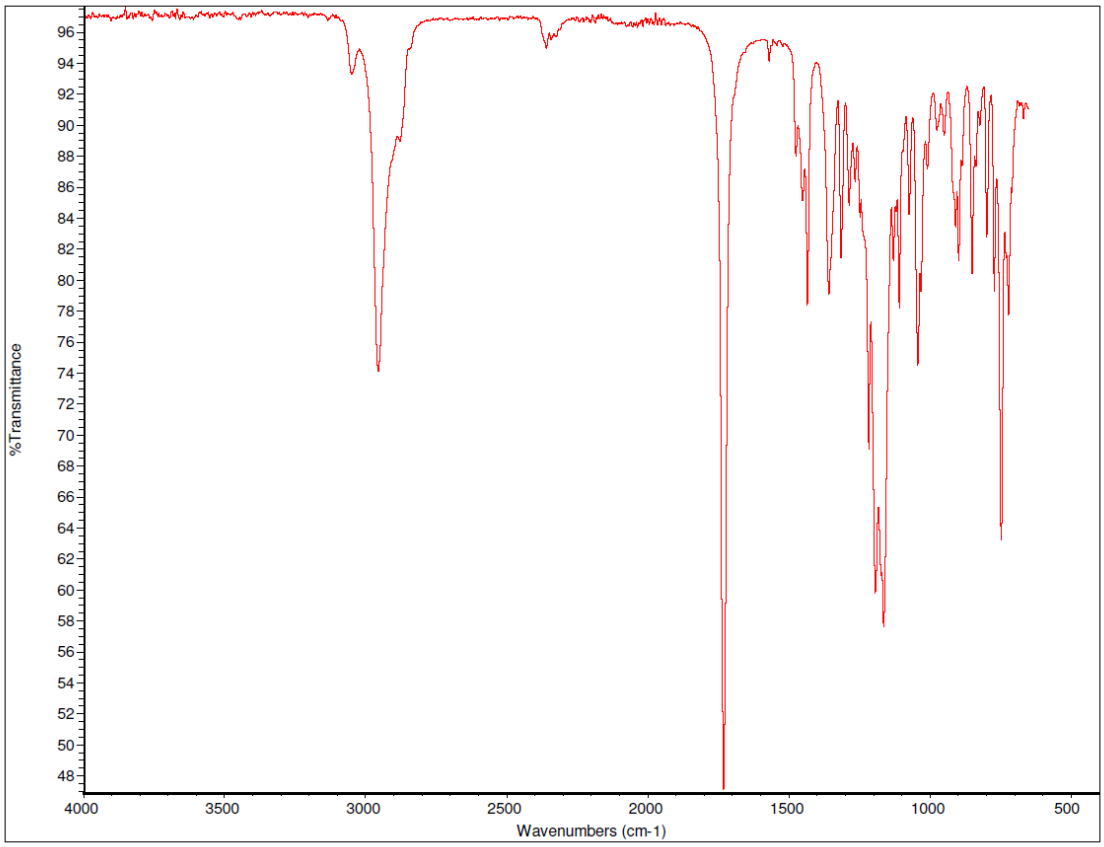

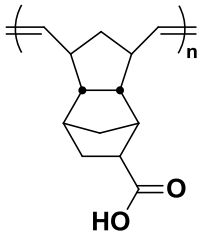

22

22. Potassium hydroxide (0.242 g, 4.313 mmol) was dissolved in 25 mL H_2O and 25 mL methanol. Upon dissolution, the homopolymer, **21**, (0.426 g, 1.952 mmol) was added, and the mixture was stirred at 50 ^{o}C overnight. Dilute hydrochloric acid was added until the mixture was strongly acidic and precipitate present. The solid was filtered, washed

with H_2O and methanol, and dried on high vacuum. The polymer was isolated as a white solid (0.400 g, 100 %).

References

1. Kim, H.-C.; Park, S.-M.; Hinsberg, W. D., Block Copolymer Based Nanostructures: Materials, Processes, and Applications to Electronics. *Chemical Reviews (Washington, DC, United States)* **2010,** *110* (1), 146-177.
2. Bates, F. S.; Fredrickson, G. H., Block copolymer thermodynamics: theory and experiment. *Annual Review of Physical Chemistry* **1990,** *41*, 525-57.
3. Albert, J. N. L.; Epps, T., Self assembly of block copolymer thin films. *Materials Today* **2010,** *13* (6), 24-33.
4. Han, E.; Stuen, K. O.; La, Y.-H.; Nealey, P. F.; Gopalan, P., Effect of Composition of Substrate-Modifying Random Copolymers on the Orientation of Symmetric and Asymmetric Diblock Copolymer Domains. *Macromolecules (Washington, DC, United States)* **2008,** *41* (23), 9090-9097.
5. Moore, G. E. *Electronics* **1965**, *38* (8).
6. http://www.deepspar.com/wp-data-loss.html. **2007**.
7. Wgsimon, "Transistor Count and Moore's Law - 2011" May 13, 2011 via Wikimedia, Creative Commons Attribution.
8. Wang, H., "Hard drive capacity over time" February 25, 2009 via Wikimedia, Creative Commons Attribution.
9. Chen, Stefanie, "Conventional Multigrain Media and Bit Patterned Media" December 5, 2012 via http://www.stuffbystef.com.
10. http://www.tomshardware.com/reviews/hitachi-7k1000-terabyte-hard-drive,1584-3.html. **2007**.
11. http://willson.cm.utexas.edu/Research/Sub_Files/Immersion/index.php. **2006**.
12. Dusa, M.; Arnold, B.; Finders, J.; Meiling, H.; Schenau, K. v. I.; Chen, A. C.; Toshiyuki, H., Ed.; *SPIE* **2008**, *7028*, 702810.
13. http://semimd.com/blog/2011/11/25/asml%E2%80%99s-euv-roadmap-points-to-new-wavelength/. **2011**.
14. http://willson.cm.utexas.edu/Research/Sub_Files/SFIL/Process/process1.bmp. **2012**.
15. Rogers, J. A. *Nano Letters*, **2004**, *4* (12), 2467-2471.
16. Yang, X., et al., *ACS Nano* **2009,** *3* (7), 1844-1858.
17. Kim, H.-C.; Park, S.-M.; Hinsberg, W. D. *Chemical Reviews (Washington, DC, United States)* **2010**, *110*, 146.
18. Cushen, J. D.; Otsuka, I.; Bates, C. M.; Halila, S.; Fort, S.; Rochas, C.; Easley, J. A.; Rausch, E. L.; Thio, A.; Borsali, R.; Willson, C. G.; Ellison, C. J. *ACS Nano* **2012**, *6*, 3424.
19. Bates, F. S.; Fredrickson, G. H., *Physics Today* **1999,** *52* (2), 32-38.
20. Reprinted (adapted) with permission from Matsen, M. W.; Bates, F. S., *Macromolecules* **1996,** *29* (4), 1091-8. Copyright 2012 American Chemical Society.

21. a) Walton, D. G.; Kellogg, G. J.; Mayes, A. M.; Lambooy, P.; Russell, T. P. *Macromolecules***1994**, *27*, 6225. b) Segalman, R. A.; Yokoyama, H.; Kramer, E. J. *Adv. Mater.***2001**, *13*, 1152. c) Park, S.; Lee, D. H.; Xu, J.; Kim, B.; Hong, S. W.; Jeong, U.; Xu, T.; Russell, T. P. *Science***2009**, *323*, 1030.
22.Ham, S.; Shin, C.; Kim, E.; Ryu, D. Y.; Jeong, U.; Russell, T. P.; Hawker, C. J. *Macromolecules***2008**, *41*, 6431.
23.Leibler, L. *Macromolecules***1980**, *13*, 1602.
24.Colburn, M.; Grot, A.; Amistoso, M. N.; Choi, B. J.; Bailey, T. C.; Ekerdt, J. G.; Sreenivasan, S. V.; Hollenhorst, J.; Willson, C. G. *Proc. SPIE-Int. Soc. Opt. Eng.***2000**, *3997*, 453.
25.Takuhei, N. *Polymer***1995**, *36*, 2243.
26. Ryu, D. Y.; Shin, K., Drockenmuller, E., Hawker, C., Russell, T. P. *Science***2005**, *308*, 236.
27. Koberstein, J.T. *Macromolecules* **2007**, *40*, 1604-1614.
28. Koberstein, J.T. *Polym. Mat. Sci. Eng.* **2001**, *84*, 343-344.
29. Houlihan, F. M.; Wallow, T. I.; Nalamasu, O.; Reichmanis, E. *Macromolecules* **1997**, *30*, 6517.
30.Haswelwander, T.A.; Heitz, W.; Krugel, S.A.; Wendorff, J.H. *Macromol.Chem. Phys.***1996**, *197*, 3435.
31.Peruch, F.; Cramail, H.; Deffieux, A. *Macromol.Chem. Phys.***1998**, *199*, 2221.
32. Goodall, B.L.; Jayaraman, S.; Shick, R.A.; Rhodes, L.F. *WO97/33198, BFGoodrich, invs.* **1997.**
33.Bullen, G.J.; Mason, R.; Pauling, P. *Nature* **1961**, *189*, 291-292.
34. http://www.ramehart.com/contactangle.htm. **2012**.
35. Lipian, J., et al. Catalyst and Methods for Polymerizing Cycloolefins. U.S. Patent 6455650 B1, Sep 24, 2002. Ex 108-110
36. Bates, C. M.; Seshimo, T.; Maher, M. J.; Durand, W. J.; Cushen, J. D.; Dean, L. M.; Blachut, G.; Ellison, C. J.; Willson, C. G. *Science* **2012**, *338*, 775-779.
37. Cowie, J. M. G. Alternating Copolymers. *Plenum Press* **1985**.